Preprint
UCRL-JRNL-205768

Apparent molar volumes and apparent molar heat capacities of $Pr(NO_3)_3(aq)$, $Gd(NO_3)_3(aq)$, $Ho(NO_3)_3(aq)$, and $Y(NO_3)_3(aq)$ at T = (288.15, 298.15, 313.15, and 328.15) K and p = 0.1 MPa

A. W. Hakin, J. L. Liu, K. Erickson, J.-V. Munoz, and J. A. Rard

This article was submitted to Journal of Chemical Thermodynamics

June 2004

DISCLAIMER

Apparent molar volumes and apparent molar heat capacities of $Pr(NO_3)_3(aq)$, $Gd(NO_3)_3(aq)$, $Ho(NO_3)_3(aq)$, and $Y(NO_3)_3(aq)$ at T = (288.15, 298.15, 313.15, and 328.15) K and p = 0.1 MPa.

Andrew W. Hakin*, Jin Lian Liu, Kristy Erickson, Julie-Vanessa Munoz

Department of Chemistry and Biochemistry, University of Lethbridge, 4401 University Drive, Lethbridge, Alberta, Canada T1K 3M4

and Joseph A. Rard

Energy and Environment Directorate, Lawrence Livermore National Laboratory, University of California, Livermore, CA 94550, U.S.A

Received ( )

* Corresponding author: Tel.: (403) 329-2083; fax: (403) 329-2057
Email address: hakin@uleth.ca

Abstract

Relative densities and relative massic heat capacities have been measured for acidified solutions (prepared at University of Lethbridge) of $Y(NO_3)_3$(aq), $Pr(NO_3)_3$(aq), and $Gd(NO_3)_3$(aq) at T = (288.15, 298.15, 313.15, and 328.15) K and p = 0.1 MPa. In addition, relative densities and massic heat capacities have been measured at the same temperatures and pressure for $Y(NO_3)_3$(aq) and $Ho(NO_3)_3$(aq) solutions which were supplied from the Lawrence Livermore National Laboratory (LLNL) (n.b. measurements at T = 328.15 K for $Ho(NO_3)_3$(aq) were not performed due to the limited volume of solution available). Apparent molar volumes and apparent molar heat capacities for the aqueous salt solutions have been calculated from the experimental apparent molar properties of the acidified salt solutions using Young's Rule whereas the apparent molar properties of the LLNL solutions were calculated directly from the measured densities and massic heat capacities. The two sets of data for the $Y(NO_3)_3$(aq) systems provide a check of the internal consistency of the Young's Rule approach we have utilised.

The concentration dependences of the apparent molar volumes and heat capacities of the aqueous salt solutions have been modelled at each investigated temperature using the Pitzer ion interaction equations to yield apparent molar properties at infinite dilution.

Complex formation within the aqueous rare earth nitrate systems is discussed and is qualitatively explored by probing the concentration dependence of apparent molar volumes and heat capacities. It is also shown that in spite of the complex formation within the aqueous rare earth nitrate systems there remains a high degree of self-consistency between the apparent molar volumes and heat capacities at infinite dilution reported in this manuscript and those previously reported for aqueous rare earth perchlorate salt systems.

Introduction

We have recently reported volumetric and thermochemical data for aqueous rare earth sulfate [1], rare earth perchlorate [2,3], and rare earth chloride [4] systems. With respect to these studies it noted that the thermodynamic properties of the perchlorates are essentially free of contributions arising from complex formation, that the contributions made by the $REECl^{2+}(aq)$ and $REECl_2^{+}(aq)$ to the thermodynamic properties of the dilute chloride systems are almost negligible, and that the thermodynamic properties of dilute aqueous sulfate systems are dominated by the formation of the $REE(SO_4)^{+}(aq)$ and $REE(SO_4)_2^{-}(aq)$ species. In this paper we turn our attention to aqueous rare earth nitrate systems in which the degree of complex formation, as judged by the magnitude of available complex formation constants (see Ref. [5] and references therein) and also the results of isopiestic [6-9] and electrical conductance measurements [10], is greater than that for the chlorides but still considerably less than that found for sulfate systems. Values for stability constants reported in the literature indicate that nitrate complex formation is more prevalent for the light rare earths than the heavy rare earths with a maximum occurring approximately at samarium [11]. Over the concentration ranges investigated in this study the mono nitrate complex, $REE(NO_3)^{2+}(aq)$, is the dominant complex species in solution; however, at higher concentrations it is likely that the species $REE(NO_3)_2^{+}(aq)$ and $REE(NO_3)_3(aq)$ will also be present. In addition, it has also been reported that a mixture of inner sphere and outer sphere complexation occurs in aqueous nitrate solutions [8].

Although there have been several previous studies which report apparent molar volumes and apparent molar heat capacities for aqueous rare earth nitrate solutions they have invariably been

restricted to T = 298.15 K and p = 0.1 MPa [11-14]. In addition, it would appear that the only previous calorimetric heat capacity investigation performed on aqueous rare earth nitrates [14] utilised the technique of batch calorimetry that has previously been shown to lack the precision of the flow calorimetry procedure used in this study when investigating dilute aqueous solutions [1-4].

This manuscript reports relative densities and relative massic heat capacities for acidified solutions of $Pr(NO_3)_3$(aq), $Gd(NO_3)_3$(aq), and $Y(NO_3)_3$(aq) at T = (288.15, 298.15, 313.15, and 328.15) K and p = 0.1 MPa. The relative properties have been used to calculate experimental apparent molar volumes and heat capacities from which the apparent molar properties of the aqueous salt solutions have been obtained through the use of Young's rule [15]. Relative densities and relative massic heat capacities have also been measured for high purity aqueous solutions of $Y(NO_3)_3$(aq) and $Ho(NO_3)_3$(aq) which were supplied from the Lawrence Livermore National Laboratory (LLNL). The latter solutions do not contain an excess of HNO_3(aq) and therefore provide a more direct route to the required apparent molar properties at infinite dilution. The densities and massic heat capacities obtained from the LLNL $Y(NO_3)_3$(aq) sample provides a good test of the reliability of the Young's Rule approach that was utilised in analysing the acidified rare earth nitrate solutions.

Experimental

Samples of acidified $Pr(NO_3)_3$(aq), $Gd(NO_3)_3$(aq), and $Y(NO_3)_3$(aq) were prepared from the relevant oxides and dilute nitric acid using a modification of the method described by Spedding *et al*. [12] that was previously utilized to prepare aqueous samples of rare earth perchlorates [2,3] and rare earth chlorides [4]. Samples of Pr_2O_3(s) (0.999 mol fraction), Gd_2O_3(s) (0.999 mol fraction), and Y_2O_3(s) (0.9999 mol fraction) were purchased from the Aldrich Chemical Company (catalogue numbers 55,824-9, 27,851-3, and 20,516-8 respectively) and were used, without further purification. The nitric acid used in these preparations was purchased from BDH Chemicals. The water used in the preparation of the

stock acidified nitrate salt solutions was obtained from a distilled water fed Osmonics model Aries High Purity De-ionized Water Loop that polishes water to a typical resistivity of 18.3 MΩ·cm. The acidified stock solutions of the aqueous nitrate salt were standardized for metal ion content and acid content using previously detailed volumetric titration procedures [2-4]. Each investigated temperature involved nine or ten sample solutions which were prepared from the stock solutions by mass using a Mettler Toledo AT201 balance. Solutions were stored in sealed 25 mL glass volumetric flasks and were used within 24 hours of their preparation.

Samples of high purity $Y(NO_3)_3$(aq) and $Ho(NO_3)_3$(aq) were obtained from LLNL. The samples were prepared from high purity oxides and the purity of the $Y(NO_3)_3$ sample was 99.951 mol% based on mass spectrometry whilst that of $Ho(NO_3)_3$ was 99.984 mol% based on d.c. arc optical emission spectroscopy, where the amounts of individual impurities detected are given by Marriott *et al*. [1]. All samples were found to contain trace amounts of other rare earths, calcium and iron. The concentration of one stock $Ho(NO_3)_3$(aq) solution was determined to be (1.0836 ± 0.0009) mol·kg^{-1} based on three gravimetric sulfate analyses and a mass titration with EDTA, whilst the concentration of a second stock solution was determined using precise density measurements at T = 298.15 K to be (0.6250 ± 0.0005) mol·kg^{-1}. The concentration of the $Y(NO_3)_3$(aq) stock solution was (1.2186 ± 0.0007) mol·kg^{-1} based on two gravimetric sulfate analyses. The densities of $Ho(NO_3)_3$(aq) used for determining the molality (0.6250 ± 0.0005) mol·kg^{-1} of the second stock solution were measure using solutions prepared by mass dilution of samples of the more concentrated stock solution. The uncertainty of 0.0005 mol·kg^{-1} was estimated by an appropriate propagation of error calculation. Sample solutions of $Ho(NO_3)_3$(aq) and $Y(NO_3)_3$(aq) for relative density and relative heat capacity measurements were prepared by mass by the dilution of these stock solutions.

The molar masses of the nitrate salts and the nitric acid used in this study were calculated using the recommendations of the 1995 Commission on Atomic Weights and Isotopic Abundances [16] $M(Pr(NO_3)_3)$ = 0.32692 kg·mol^{-1}, $M(Gd(NO_3)_3)$ = 0.34326 kg·mol^{-1}, $M(Ho(NO_3)_3)$ = 0.35094_5 kg·mol^{-1}, $M(Y(NO_3)_3)$ = 0.27492 kg·mol^{-1}, $M(HNO_3)$ = 0.063013 kg·mol^{-1}.

Relative density, ($\rho - \rho_1$), measurements were made with a Sodev 02D Vibrating Tube Densimeter. Details of the setup and operation of the densimeter have been previously reported in detail [1], however it is noted that the calculation of the calibration constant of the instrument at each investigated temperature required densities for air, ρ, [17] and pure water (ρ_1 = (999.101, 997.047, 992.219, and 985.695) kg·m^{-3} at T = (288.15, 298.15, 313.15, and 328.15) K and p = 0.1 MPa, respectively) [18]. The uncertainty in density introduced by the Sodev instrument is estimated to be $5 \cdot 10^{-3}$ kg·m^{-3} and as such is somewhat less than the uncertainty contribution associated with the concentrations of the acidified sample solutions.

A Picker Flow Microcalorimeter was connected in series with the densimeter and was used to measure the volumetric heat capacities of the sample solutions. Details of the setup and operation of the calorimeter have also been previously described in detail [1]. However, it is noted that a value of f = 1.0106 ± 0.0076 was used as the heat leak correction factor [19] for the calorimeter at all investigated temperatures. The uncertainty associated with relative massic heat capacities obtained from the calorimeter is estimated to be $7 \cdot 10^{-5}$ J·K^{-1}·g^{-1} and is once again somewhat less than the uncertainty associated with the concentrations of the acidified nitrate salt solution samples.

Experimental Apparent Molar Properties

The apparent molar volumes of the acidified nitrate salt solutions, $V_{\phi,expt}$, were calculated from relative densities using the equation:

$$V_{\phi,expt} = [\{((1 + m_2 \cdot M_2 + m_3 \cdot M_3)/\rho_{expt}) - (1/\rho_1)\}/(m_2 + m_3)]. \quad (1)$$

where m_2 and m_3 are the molalities, and M_2 and M_3 the molar masses of the rare earth nitrate salts and nitric acid, respectively. The apparent molar heat capacities of the acidified nitrate solutions, $C_{p\phi,expt}$, were calculated in a similar manner using the equation:

$$C_{p\phi,expt} = [\{(1 + m_2 \cdot M_2 + m_3 \cdot M_3) \cdot c_{pexpt} - c_{p1}\}/(m_2 + m_3)], \quad (2)$$

where c_{pexpt} and c_{p1} are the massic heat capacities of the solution and of pure water, respectively. Massic heat capacities for pure water were obtained from the tabulations reported by Stimson [20] {c_{p1} = (4.1855, 4.1793, 4.1783, and 4.1821) $J \cdot K^{-1} \cdot g^{-1}$ at T = (288.15, 298.15, 313.15, and 328.15) K, respectively}.

The apparent molar properties of the aqueous nitrate salt solutions, $Y_{\phi,2}$, were obtained from the experimental apparent molar properties of the acidified solutions using Young's Rule [15].

$$[m_2/(m_2 + m_3)] \cdot Y_{\phi,2} = Y_{\phi,expt} - [m_3/(m_2 + m_3)] \cdot Y_{\phi,3} - \delta. \quad (3)$$

In this equation, Y is used to identify the apparent molar thermodynamic property of interest at the total ionic strength of the mixed electrolyte solution and δ identifies an excess mixing term that was assumed to be equal to zero in all of our calculations [2-4]. Values for the apparent molar volumes and heat capacities of aqueous nitric acid solutions, $Y_{\phi,3}$, were calculated from equations reported by Hovey [21]. These equations model the concentration and temperature dependences of the apparent molar volumes and heat capacities of dilute solutions of HNO_3(aq) at p = 0.1 MPa and the temperature range $283.15 \leq T/K \leq 328.15$. Tables 1 to 3 report the concentration and temperature dependences of the relative

densities, relative massic heat capacities, and apparent molar volumes and heat capacities for the investigated acidified aqueous solutions of $Pr(NO_3)_3$(aq), $Gd(NO_3)_3$(aq), and $Y(NO_3)_3$(aq), respectively.

The apparent molar volumes of the LLNL $Ho(NO_3)_3$(aq), and $Y(NO_3)_3$(aq) solutions were calculated using the standard relation:

$$V_{\phi,2} = (M_2/\rho) - \{(\rho_{expt} - \rho_1)/m_2 \cdot \rho_{expt} \cdot \rho_1\}. \quad (4)$$

The apparent molar heat capacities of the solutions were calculated using the relation:

$$C_{p\phi,2} = (M_2 \cdot c_{pexpt}) + \{(c_{pexpt} - c_{p1})/m_2\}. \quad (5)$$

Tables 4 and 5 report the concentration and temperature dependences of the experimentally determined relative densities and relative massic heat capacities as well as the calculated apparent molar volumes and heat capacities for the LLNL $Ho(NO_3)_3$(aq) and $Y(NO_3)_3$(aq) solutions, respectively.

The uncertainties in the experimental apparent molar values, $\delta Y_{\phi,expt}$, which are reported in tables 1-5 were estimated using previously described methods [1,4].

As indicated above, previously reported volumetric studies on aqueous rare earth nitrate systems have been limited to T = 298.15 K and p = 0.1 MPa. Two of these previous studies utilized magnetically controlled floats [11,12] to provide precise densities for aqueous solutions of the nitrate salts of La, Nd, Er, and Yb [12] and also Pr, Sm, Eu, Gd, Tb, Dy, Ho, Tm, and Lu [11] at T = 298.15 K in the approximate concentration range of $0.0015 < m_2/(\text{mol}\cdot\text{kg}^{-1}) < 0.2$. Although reference [11] only reports parameters for equations which model the concentration dependences of the calculated apparent molar volumes rather than the experimentally determined densities, they are available as supplementary material from the American Chemical Society. However, measured densities are contained in the

pycnometric study reported by Spedding *et al*. [13]. The latter manuscript reports densities and apparent molar volumes for aqueous solutions of the nitrate salts of La, Pr, Nd, Sm, Gd, Tb, Dy, Ho, Er, Yb, and Lu in the concentration range of approximately 0.03 $mol \cdot kg^{-1}$ to saturation and provides a useful comparison with $V_{\phi,2}$ values reported in this manuscript. Figure 1 shows a plot of the concentration dependence of the apparent molar volumes for $Pr(NO_3)_3(aq)$ obtained in this study at T = 298.15 K compared with those values reported in references [11] and [13]. The figure indicates excellent agreement between the values obtained in this study and those reported in reference [13]; however, the values obtained from the supplementary material associated with reference [11] are approximately 1 $cm^3 \cdot mol^{-1}$ lower than the other investigations. Good agreement is observed for the $V_{\phi,2}$ data reported in table 4 at T = 298.15 K for the $Ho(NO_3)_3(aq)$ system and those reported in reference [13]. It is noted however that the $V_{\phi,2}$ values obtained in this study for $Gd(NO_3)_3(aq)$ at T = 298.15 K are approximately 1 $cm^3 \cdot mol^{-1}$ lower than those reported in reference [13].

Densities and apparent molar volumes for $Y(NO_3)_3(aq)$ have been previously reported by Rard and Spedding [9] at T = 298.15 K and p = 0.1 MPa. These measurements were made with a matched pair of single stem pycnometers with an accuracy of 3 x 10^{-2} $kg \cdot m^3$. Figure 2 provides a comparison of the two sets of $V_{\phi,2}$ values for $Y(NO_3)_3(aq)$ obtained in this study with those previously reported in reference [9]. Excellent agreement is observed between all three sets of data.

The adiabatic single can calorimeter study of Spedding, Baker, and Walters [14] reports apparent molar heat capacities for aqueous solutions of the nitrate salts of La, Pr, Nd, Sm, Gd, Tb, Dy, Ho, Er, Tm, Yb, and Lu at T = 298.15 K and p = 0.1 MPa in the concentration range $0.09 < m_2 / (mol \cdot kg^{-1}) \leq m_2(sat)$, where $m_2(sat)$ is the molality of the saturated solution. Reference [14] appears to be the only previous calorimetric study of aqueous rare earth nitrate systems to have been reported in the literature that reports the apparent molar heat capacities of aqueous rare earth nitrate solutions. Plots of the concentration dependences of the apparent molar heat capacities for $Pr(NO_3)_3(aq)$ and $Gd(NO_3)_3(aq)$

indicate that there is good agreement between the current study and reference [14]. There appear to be no previous studies in the literature which report apparent molar heat capacities for the $Y(NO_3)_3$(aq) system.

Modelling of Apparent Molar Properties

The calculated apparent molar volumes of each aqueous salt system were modelled at each temperature using a truncated form of the Pitzer ion interaction equations [22]. For the trivalent metal cation containing nitrate salts investigated in this paper the Pitzer ion interaction equation takes the form:

$$V_{\phi,2} = V_2^{o} + (6 \cdot A_v/b) \cdot \ln(1+b \cdot I^{1/2}) + 6 \cdot R \cdot T \cdot m_2 \cdot \beta^{0V} + 12 \cdot R \cdot T \cdot m_2 \cdot f(I) \cdot \beta^{1V}. \quad (6)$$

In this equation, V_2^{o}, is the apparent molar volume of the aqueous salt solution at infinite dilution, I is the total ionic strength of the system, R is the universal gas constant (8.31451 $J \cdot K^{-1} \cdot mol^{-1}$), and b = 1.2 $kg^{1/2} \cdot mol^{-1/2}$. Values for the Debye-Hückel limiting slope A_v at each temperature T and p = 0.1 MPa were obtained from the tables reported by Archer and Wang [23] and the ionic strength function $f(I)$ was calculated using the equation:

$$f(I) = [1 - \{(1+a \cdot I^{1/2}) \cdot \exp(-a \cdot I^{1/2}\}]/(a^2 \cdot I), \quad (7)$$

where a = 2.0 $kg^{1/2} \cdot mol^{-1/2}$.

Values for the fitting constants β^{0V} and β^{1V} were obtained using multiple regression analyses and are reported with together with V_2^{o} values and all of the associated standard errors in table 6.

The temperature dependences of the V_2^o values obtained from the use of equation (6) may be modelled using an empirical equation of the form:

$$V_2^o = a + b\cdot(T - 308.15) + c\cdot(T - 308.15)^2. \quad (8)$$

In this equation the constant T = 308.15 K identifies the midpoint of the investigated temperature range and values of fitting coefficients a, b, and c are obtained by fitting equation (8) to the values of V_2^o for each aqueous rare earth nitrate salt system using weighted regression analyses. The weights used in these analyses were calculated as the inverse squares of the standard errors associated with the V_2^o values reported in table 6. Values for the fitting coefficients to equation (8) and their standard errors are contained in table 7. Unfortunately these calculations could not be applied to the $Ho(NO_3)_3$(aq) because the volumetric data were restricted to only three temperatures.

The first derivative of equation (8) with respect to temperature at constant pressure yields an expression for the temperature dependence of the apparent molar expansibility at infinite dilution, E_2^o ($E_2^o = (\partial V_2^o/\partial T)_p$). Values for E_2^o are easily calculated using the values of the b and c coefficients reported in table 7 as can values for T_{max}. T_{max} values identify temperatures at which maxima in values for V_2^o are observed. For $Pr(NO_3)_3$(aq), $Gd(NO_3)_3$(aq), $Y(NO_3)_3$(aq), and $Y(NO_3)_3$(aq)(LLNL) these values are calculated to be T_{max} = (325.8, 334.2, 325.5, and 323.5) K respectively. Although the two values for $Y(NO_3)_3$(aq) are in reasonable agreement with each other the calculations clearly illustrate how small variations in apparent molar volume at infinite dilution as a function of temperature can result in much larger variations within the derivative property.

The calculated apparent molar heat capacities of the aqueous salt solutions were modelled at each investigated temperature in a similar manner to $V_{\phi,2}$ values using a Pitzer ion interaction equation. This equation takes the form:

$$C_{p\phi,2} = C_{p2}^{o} + (6 \cdot A_J/b) \cdot \ln(1+b \cdot I^{1/2}) - 6 \cdot R \cdot T^2 \cdot m_2 \cdot \beta^{0J} - 12 \cdot R \cdot T^2 \cdot m_2 \cdot f(I) \cdot \beta^{1J}, \quad (9)$$

where C_{p2}^{o} is the apparent molar heat capacity of the solution at infinite dilution, and A_J is a Debye-Hückel limiting slope at temperature T /K and p = 0.1 MPa [23].

Values for the fitting constants β^{0V}, β^{1V}, β^{0J} and β^{1J} were obtained using multiple regression analyses and are reported with values for the apparent molar properties at infinite dilution and all standard errors in table 6. A comparison with previously reported V_2^{o} and C_{p2}^{o} values at T = 298.15 K and p = 0.1 MPa is presented in table 8. The value for V_2^{o} obtained in this study for $Pr(NO_3)_3$(aq) at T = 298.15 K is somewhat larger than those reported previously by Spedding *et al*. [11,13]. It is noted however that it is within ~1 $cm^3 \cdot mol^{-1}$ of the value reported by Marriott et al. [1] who did not report new volumetric data for this system but rather reanalyzed values reported by Spedding *et al*. [11,13] using an extended Debye-Hückel equation. V_2^{o} values for the $Gd(NO_3)_3$(aq) and $Ho(NO_3)_3$(aq) obtained in this study are similarly within ~ 1 $cm^3 \cdot mol^{-1}$ of previously reported values. Unfortunately, the V_2^{o} value for $Y(NO_3)_3$(aq) at T = 298.15 K that can be calculated from the Pitzer type model reported by Galas *et al*. [24] is in very poor agreement with those values obtained in this study and does not correlate well with the values for apparent molar volume reported by Rard and Spedding [9]. However, the measurements of Galas *et al*. were made at molalities $m_2 \geq 0.297$ $mol \cdot kg^{-1}$, which do not extend to low enough concentrations to yield a reliable value of V_2^{o}.

The C_{p2}^{o} values reported in table 8 from this study for $Pr(NO_3)_3$(aq), $Gd(NO_3)_3$(aq) and $Ho(NO_3)_3$ are observed to be more negative than those values reported by Spedding, Baker and Walters [14] by 20 to 40 $J \cdot K^{-1} \cdot mol^{-1}$. Reasons for this have been previously explored [2,4] and relate to the lower precision offered by batch calorimeters, of the type used by Spedding *et al*. [14], when investigating dilute aqueous solutions. It is interesting however, that Criss and Millero's [25] reanalysis

of apparent molar heat capacities of aqueous rare earth salt solutions at 298.15 K produced C_{p2}^{o} values for $Pr(NO_3)_3(aq)$ and $Gd(NO_3)_3(aq)$ which are in good agreement with those reported in this study. Such agreement is not extended to the $Ho(NO_3)_3(aq)$ system. Marriott *et al*. [1] previously pointed out that the C_{p2}^{o} value reported by Criss and Millero for $Ho^{3+}(aq)$ is inconsistent (too negative) by ≈ 20 $J \cdot K^{-1} \cdot mol^{-1}$ with values for the neighbouring rare earths.

The apparent molar volumes and heat capacities of each aqueous salt solution were modeled over the complete investigated temperature surface using modified Pitzer ion interaction equations [2-4]. In these equations the temperature dependences of the apparent molar properties at infinite dilution are modelled using the revised Helgeson, Kirkham, and Flowers (HKF) equations proposed by Tanger and Helgeson [26] and the temperature dependences of the β fitting coefficients are modelled using simple empirical equations. For apparent molar volumes the required temperature dependent equations take the form:

$$V^{o}_{2} = \upsilon_1 + (\upsilon_2/(T - \theta)) - \omega \cdot Q, \tag{10}$$

$$\beta^{0V} = \upsilon_3 + \upsilon_4 \cdot T, \tag{11}$$

$$\beta^{1V} = (\upsilon_5/T) + \upsilon_6 + \upsilon_7 \cdot T. \tag{12}$$

In equation (10) the solvent dependent parameter θ is assigned a value of T = 228 K, Q is a Born function that depends upon the pressure dependence of the dielectric constant of the solvent and ω defines a Born coefficient that is specific to the salt under study. Values for ω used in these fits were calculated from the compilation of single ion values reported by Shock and Helgeson [27]. Values for Q were calculated using equations for the dielectric constant of water reported by Johnson and Norton [28] ($10^7 \cdot Q$ = (6.49, 6.69, 7.17, and 7.88) bar^{-1} at T = (288.15, 298.15. 313.15. and 328.15) K, respectively). Values for the fitting parameters υ_i (i = 1 to 7) shown in equations (10) to (12) were obtained using multiple regression analyses and are reported in table 9. A plot of the dependent variable $V_{2,\phi}$ –

$(6 \cdot A_v/b) \cdot \ln(1+bI^{1/2}) + \omega Q$ versus the square root of the ionic strength, $I^{1/2}$, is shown for the $Pr(NO_3)_3(aq)$ system as figure 3.

The temperature dependences of calculated $C_{p2,\phi}$ values were modelled by modifying equation (9) such that:

$$C_p^{o}{}_2 = c_1 + (c_2/(T - \theta)^2) + \omega \cdot T \cdot X, \quad (13)$$

$$\beta^{0J} = (c_3/T) + c_4 + c_5 \cdot T, \quad (14)$$

and

$$\beta^{1J} = (c_6/T) + c_7 + c_8 \cdot T. \quad (15)$$

Values for the Born function X, contained in equation (13), depend upon the dielectric constant of the solvent water and were calculated using equations reported by Johnson and Norton [28] ($10^7 \cdot X$ = (–3.2, –3.1, –3.1, and –3.2) K^{-2} at T = (288.15, 298.15. 313.15. and 328.15) K, respectively). Values for the fitting parameters shown in equations (13) to (15) c_i(i = 1 to 8) were obtained through regression analyses and are reported together with their calculated uncertainties in table 10. A plot of the dependent variable $C_{p2,\phi} - (6 \cdot A_J/b) \cdot \ln(1+bI^{1/2}) - \omega TX$ versus the square root of the ionic strength, $I^{1/2}$, is shown for the $Ho(NO_3)_3(aq)$ system as figure 4.

The Effects of Complex Formation.

Trends in mean molal activity coefficients and water activities for aqueous rare earth nitrates when plotted against the ionic radii of the rare earth ions at T = 298.15 K have been found to be different from those trends obtained for the aqueous rare earth chlorides and perchlorates [6-9]. Such differences are believed to be indicative of a higher degree of complex formation within the rare earth nitrate systems. With regards to the extent of complex formation the same trends indicate that complex formation increases with decreasing cationic radius from $La(NO_3)_3(aq)$ to around $Sm(NO_3)_3(aq)$ and then

decreases with further decreases in ionic radius to $Lu(NO_3)_3(aq)$. Based on this information one would expect the degree of complex formation in $Ho(NO_3)_3(aq)$ and $Gd(NO_3)_3(aq)$ to be lower than that observed in aqueous solutions of $Pr(NO_3)_3$. The ionic radius of Y^{3+} falls between that Er^{3+} and Tm^{3+} within the lanthanide series and values for mean molal activity coefficients and water activities for $Y(NO_3)_3(aq)$ would also appear to indicate that it forms lower order complexes in aqueous solution. However, at higher concentrations it is likely that higher order complexes in $Y(NO_3)_3(aq)$ solutions are less stable than those for the lanthanide nitrates.

The electrical conductances reported by Rard and Spedding [10] for aqueous rare earth nitrate solutions at T = 298.15 K also support the conclusions drawn from the isopiestic measurements described above. We also note that the $V_{\phi,2}$ values of the $REECl_3(aq)$, $REE(ClO_4)_3(aq)$, and of most of the $REE(NO_3)_3(aq)$ are well represented by the Owen-Brinkley equation [11,12] (which is an extended Debye-Hückel equation). However, the $V_{\phi,2}$ values for $Nd(NO_3)_3(aq)$ show significant deviations from this equation, which presumably results from a greater degree of complex formation compared to the other $REE(NO_3)_3(aq)$.

A qualitative method of confirming the higher degree of complex formation within aqueous rare earth nitrate salt solutions relative to the assumed negligible complex formation with rare earth perchlorate salt solutions is to look at the concentration dependences of the differences $V_{2,\phi} - V_2^{o}$ and $C_{p2,\phi} - C_{p2}^{o}$. In such plots one would expect the concentration dependence of the apparent molar property of a complexed rare earth system to be greater than that of a non-complexed solution of the perchlorate salt of the same rare earth species. This approach has been previously utilised to explore the degree of complex formation within aqueous rare earth chloride [4] and aqueous rare earth sulfate [1] systems. Figure 5 shows a plot of $V_{2,\phi} - V_2^{o}$ against the square root of the total ionic strength for $Pr(NO_3)_3(aq)$ and $Pr(ClO_4)_3(aq)$ at T = 298.15 K. The figure clearly indicates that values for $V_{2,\phi} - V_2^{o}$ are larger and more positive for the nitrate salt than for the perchlorate salt. A similar observation is

made in figure 6 that shows a plot of $C_{p2,\phi} - C_{p2}^{o}$ against the square root of ionic strength for $Pr(NO_3)_3(aq)$ and $Pr(ClO_4)_3(aq)$ at T = 298.15 K. Similar behaviour is observed at the other temperatures investigated in this study. Volume and heat capacity difference plots for the other rare earth nitrates studied in this investigation and the perchlorates follow the same pattern as that observed for $Pr(NO_3)_3(aq)$ and $Pr(ClO_4)_3(aq)$. On closer inspection however it is also noted that the $V_{2,\phi} - V_2^{o}$ and $C_{p2,\phi} - C_{p2}^{o}$ values calculated for $Y(NO_3)_3(aq)$, $Ho(NO_3)_3(aq)$, and $Gd(NO_3)_3(aq)$ are closer to those of the rare earth perchlorate salts than those for $Pr(NO_3)_3(aq)$ and $Pr(ClO_4)_3(aq)$. These observations provide further support for the conclusions drawn from the earlier isopiestic measurements that were discussed above.

In terms of the single ion volumes and heat capacities that can calculated from the reported apparent molar properties at infinite dilution reported in table 6 using the $V_2^{o}(H^+) = 0$ and $C_{p2}^{o}(H^+) = 0$ conventions one would expect the values obtained for $V_2^{o}(Ho^{3+})$, $C_{p2}^{o}(Ho^{3+})$, $V_2^{o}(Gd^{3+})$, $C_{p2}^{o}(Gd^{3+})$, $V_2^{o}(Y^{3+})$, $C_{p2}^{o}(Y^{3+})$, to be close in value to those values calculated from perchlorate salt and even chloride salt data. Although aqueous solutions of $Pr(NO_3)_3(aq)$ are thought to have an increased level of complex formation relative to the other nitrate salts investigated in this study it is also likely that the modelling of the apparent molar properties of this system will remain highly dependent on electrostatic interactions and not on the effects of complex formation. Therefore it is probable that the Pitzer ion-interaction model used in this study will yield apparent molar properties at infinite dilution for $Pr(NO_3)_3(aq)$ which are in reasonable agreement with those obtained for the perchlorate salt. An indication of the self consistency of our volumetric and thermochemical data for the rare earth perchlorate [2,3] and nitrate salts may be obtained by examining data for pairs of salts containing a common rare earth cation. In this approach the temperature dependences of values for $V_2^{o}(NO_3^-) - V_2^{o}(ClO_4^-)$ and $C_{p2}^{o}(NO_3^-) - C_{p2}^{o}(ClO_4^-)$ are calculated for $Ho(NO_3)_3/Ho(ClO_4)_3$, $Gd(NO_3)_3/Gd(ClO_4)_3$, $Y(NO_3)_3/Y(ClO_4)_3$, and $Pr(NO_3)_3/Pr(ClO_4)_3$ and are compared to those values calculated from the

infinite dilution apparent molar properties of the parent acids HNO_3/$HClO_4$ [21]. If the data sets are self-consistent then one should observe good agreement between the salt data and those obtained for the acids. Figure 7 shows the temperature dependences of calculated $V_2^o(NO_3^-) - V_2^o(ClO_4^-)$ values whilst figure 8 reports the temperature dependences of calculated $C_{p2}^o(NO_3^-) - C_{p2}^o(ClO_4^-)$ values. The error bars shown on these plots refer only to the uncertainties associated with the parent acids however it is noted that values for the salts are in agreement with the acid values within the sum of the combined uncertainties. Such plots indicate a high level of self-consistency within our data sets.

Although in principal it should be possible to model the speciation within the rare earth nitrate systems in a similar manner to that described previously with respect to aqueous rare earth sulfate systems, in practice these procedures are made slightly more complicated by the small amounts of excess acid used in the preparation of our solutions. In addition, it appears that reliable and consistent formation constant data required for these calculations are only available at T = 298.15 K [5]. Therefore, the modelling of the speciation within the investigated rare earth nitrates will not be pursued further at the current time.

In conclusion, although the temperature dependences of apparent molar volumes and heat capacities remain unknown for the majority of aqueous rare earth nitrate solutions, they will most likely not become the subject of future investigations form this laboratory due to the relatively small (compared to sulfate salts) but significant levels of complex formation found within the solutions. In probing the higher temperature and pressure thermodynamic properties of trivalent metal cations in aqueous solution our attention will be directed instead towards further investigations on aqueous perchlorate salts and also the triflate salts.

Acknowledgement

A.W. H. is grateful to the Natural Sciences and Engineering Research Council of Canada (NSERC) for the award of an individual operating grant. The contributions of J. A. R. were supported under the auspices of the Office of Basic Energy Sciences (Geosciences) under the auspices of the U. S. Department of Energy by University of California, Lawrence Livermore National Laboratory under contract No. W-7405-ENG-48.

References

[1] R.A. Marriott, A.W. Hakin, J.A. Rard, J. Chem. Thermodyn. 33 (2001) 643-687.

[2] A.W. Hakin, M.J. Lukacs, J.L. Liu, K. Erickson, A. Madhavji, J. Chem. Thermodyn. 35 (2003), 775-802.

[3] A.W. Hakin, M.J. Lukacs, J.L. Liu, J.Chem. Thermodyn. (2004), in press.

[4] A.W. Hakin, M.J. Lukacs, J.L. Liu, K. Erickson, J. Chem. Thermodyn. 35 (2003) 1861-1895.

[5] C. Bonal, J-P. Morel, N. Morel-Desrosiers, J. Chem. Soc. Faraday Trans. 94 (1998) 1431-1436.

[6] J.A. Rard, L.E. Shiers, D.J. Heiser, F.H. Spedding, J. Chem. Eng. Data 22 (1977) 337-347.

[7] J.A. Rard, D.G. Miller, F.H. Spedding, J. Chem. Eng. Data 24 (1979) 348-354.

[8] J.A. Rard, F.H. Spedding, J. Chem. Eng. Data 26 (1981) 391-395.

[9] J.A. Rard, F.H. Spedding, J. Chem. Eng. Data 27, (1982), 454-461.

[10] J.A. Rard, F.H. Spedding, J. Phys. Chem., 79 (1975) 257-262.

[11] F.H. Spedding, P.F. Cullen, A. Habenschuss, J. Phys. Chem., 78 (1974) 1106-1110.

[12] F.H. Spedding, M. J. Pikal, B.O. Ayers, J. Phys. Chem., 70 (1966) 2440-2449.

[13] F.H. Spedding, L.E. Shiers, M.A. Brown, J.L. Baker, L. Guitierrez, L.S. McDowell, A. Habenschuss, J. Phys. Chem., 79 (1975) 1087-1096.

[14] F.H. Spedding, J.L. Baker, J.P. Walters, J. Chem. Eng. Data 24 (1979) 298-305.

[15] T.F. Young, M.B. Smith, J. Phys. Chem. 58 (1954) 716-724.

[16] T.B. Coplen, Pure Appl. Chem. 68 (1996) 2339-2359.

[17] R.C. Weast (editor), CRC Handbook of Chemistry and Physics: 48th edition. The Chemical Rubber Co., Cleveland, OH. (1967).

[18] G.S. Kell, J. Chem. Eng. Data 12 (1967) 66-69.

[19] J.E. Desnoyers, C. de Vissier, G. Perron, P. Picker, J. Solution Chem. 5 (1976) 605-616.

[20] H.F. Stimson, Am. J. Phys., 23 (1955) 614-622.

[21] J.K. Hovey, PhD Thesis, The University of Alberta, Canada, (1988).

[22] K.S. Pitzer, Activity Coefficients in Electrolyte Solutions, second ed., CRC Press, Boca Raton, FL, (1991).

[23] D.G. Archer, P.Wang, J. Phys. Chem. Ref. Data 19 (1990) 371-411.

[24] O.V. Galas, S.L. Lyubimov, B.R. Churagulov, Russ. J. Phys. Chem., 67 (1993) 20-24.

[25] C.M. Criss, F.J. Millero, J. Solution Chem., 28 (1999) 849-864.

[26] J.C. Tanger IV, H.C. Helgeson, Am. J. Sci., 288 (1988) 19-98.

[27] E.L. Shock, H.C. Helgeson, Geochim. Cosmochim. Acta 52 (1988) 2009-2036.

[28] J.W. Johnson, D. Norton, Am. J. Sci. 291 (1991) 541-648.

TABLE 1 The concentration dependences of relative densities, relative heat capacities, apparent molar volumes and apparent molar heat capacities for acidified aqueous solutions of $Pr(NO_3)_3$ at T = (288.15, 298.15, 313.15, and 328.15) K.

m_2 mol·kg^{-1}	m_3 mol·kg^{-1}	$\rho_{expt} - \rho_1$ kg·m^{-3}	$V_{\phi expt}$ cm^3·mol^{-1}	$V_{\phi 2}$ cm^3·mol^{-1}	$c_{p\,expt} - c_{p1}$ J·K^{-1}·g^{-1}	$C_{p\phi,expt}$ J·K^{-1}·mol^{-1}	$C_{p\phi 2}$ J·K^{-1}·mol^{-1}
T = 288.15 K							
0.01651	0.00176	4.679	44.93 ± 0.49	46.67 ± 0.53	-0.02831	-296.4 ± 4.5	-319.4 ± 5.0
0.03280	0.00349	9.251	46.00 ± 0.43	47.84 ± 0.47	-0.05507	-272.1 ± 3.1	-293.0 ± 3.7
0.04937	0.00525	13.865	46.86 ± 0.41	48.77 ± 0.46	-0.08140	-252.7 ± 2.7	-272.0 ± 3.3
0.06462	0.00687	18.085	47.53 ± 0.40	49.51 ± 0.45	-0.10516	-240.5 ± 2.5	-258.8 ± 3.2
0.08277	0.00880	23.078	48.24 ± 0.40	50.29 ± 0.45	-0.13307	-231.0 ± 2.4	-248.8 ± 3.1
0.09996	0.01063	27.790	48.73 ± 0.40	50.82 ± 0.44	-0.15889	-222.4 ± 2.3	-239.6 ± 3.1
0.11591	0.01233	32.144	49.12 ± 0.39	51.26 ± 0.44	-0.18238	-215.0 ± 2.3	-231.8 ± 3.0
0.13321	0.01417	36.853	49.48 ± 0.39	51.64 ± 0.44	-0.20717	-206.0 ± 2.3	-222.1 ± 3.0
0.15126	0.01609	41.734	49.91 ± 0.39	52.11 ± 0.43	-0.23252	-197.3 ± 2.2	-212.9 ± 3.0
0.16896	0.01797	46.530	50.13 ± 0.38	52.36 ± 0.43	-0.25710	-190.6 ± 2.2	-205.7 ± 3.0
T = 298.15 K							
0.01679	0.00179	4.689	48.33 ± 0.49	50.30 ± 0.53	-0.02775	-242.3 ± 4.4	-261.6 ± 4.9
0.03221	0.00343	8.947	49.45 ± 0.42	51.52 ± 0.47	-0.05209	-217.5 ± 3.0	-234.6 ± 3.6
0.04841	0.00515	13.394	50.22 ± 0.41	52.36 ± 0.46	-0.07709	-202.4 ± 2.6	-218.4 ± 3.3
0.06545	0.00696	18.046	50.81 ± 0.40	53.01 ± 0.45	-0.10273	-189.6 ± 2.4	-204.6 ± 3.1
0.08148	0.00867	22.399	51.35 ± 0.40	53.61 ± 0.44	-0.12642	-180.3 ± 2.3	-194.6 ± 3.1
0.09886	0.01051	27.098	51.81 ± 0.39	54.11 ± 0.44	-0.15150	-170.6 ± 2.3	-184.2 ± 3.0
0.11609	0.01235	31.737	52.21 ± 0.39	54.55 ± 0.44	-0.17627	-165.4 ± 2.2	-178.7 ± 3.0
0.13332	0.01418	36.366	52.52 ± 0.39	54.89 ± 0.43	-0.19996	-155.0 ± 2.2	-168.3 ± 3.0
0.15097	0.01606	41.070	52.92 ± 0.38	55.33 ± 0.43	-0.22394	-148.1 ± 2.1	-160.1 ± 2.9
0.16896	0.01797	45.882	53.10 ± 0.38	55.53 ± 0.43	-0.24811	-141.9 ± 2.1	-153.5 ± 2.9
T = 313.15 K							
0.01647	0.00175	4.551	49.98 ± 0.49	51.99 ± 0.53	-0.02628	-190.6 ± 4.5	-206.2 ± 4.9
0.03327	0.00354	9.125	51.62 ± 0.42	53.79 ± 0.47	-	-	-
0.04858	0.00517	13.266	52.51 ± 0.41	54.77 ± 0.45	-0.07479	-154.0 ± 2.6	-166.6 ± 3.2
0.06572	0.00699	17.852	53.54 ± 0.40	55.91 ± 0.45	-0.09975	-142.0 ± 2.4	-153.6 ± 3.1
0.08163	0.00868	22.132	53.80 ± 0.39	56.19 ± 0.44	-0.12245	-132.8 ± 2.3	-143.7 ± 3.0
0.09869	0.01050	26.652	54.51 ± 0.39	56.97 ± 0.44	-0.14617	-122.9 ± 2.2	-133.0 ± 3.0
0.11485	0.01222	30.929	54.97 ± 0.39	57.47 ± 0.44	-0.16835	-115.6 ± 2.2	-125.2 ± 2.9
0.13436	0.01429	36.091	55.30 ± 0.38	57.84 ± 0.43	-0.19449	-107.0 ± 2.1	-116.0 ± 2.9
0.15134	0.01610	40.579	55.47 ± 0.38	58.03 ± 0.43	-0.21670	-99.6 ± 2.1	-108.0 ± 2.9
0.16896	0.01797	45.192	55.82 ± 0.38	58.41 ± 0.43	-0.23940	-92.9 ± 2.1	-100.8 ± 2.9
T = 328.15 K							
0.01631	0.00173	4.439	52.50 ± 0.49	54.71 ± 0.53	-0.02546	-157.4 ± 4.5	-170.1 ± 4.9
0.03248	0.00345	8.789	53.70 ± 0.43	56.03 ± 0.47	-0.04970	-137.0 ± 2.9	-147.9 ± 3.5
0.04873	0.00518	13.128	54.58 ± 0.41	56.99 ± 0.45	-0.07334	-121.3 ± 2.5	-130.9 ± 3.2

0.06494	0.00691	17.434	55.19 ± 0.40	57.65 ± 0.45	-0.09655	-111.9 ± 2.3	-120.8 ± 3.1
0.08180	0.00870	21.892	55.72 ± 0.40	58.24 ± 0.44	-0.12000	-101.0 ± 2.2	-109.0 ± 3.0
0.09920	0.01055	26.465	56.22 ± 0.39	58.79 ± 0.44	-0.14398	-94.2 ± 2.2	-101.8 ± 2.9
0.11644	0.01238	30.977	56.67 ± 0.39	59.27 ± 0.44	-0.16698	-85.4 ± 2.1	-92.4 ± 2.9
0.13131	0.01397	34.866	56.89 ± 0.39	59.52 ± 0.43	-0.18672	-80.5 ± 2.1	-87.2 ± 2.9
0.15009	0.01596	39.748	57.25 ± 0.38	59.92 ± 0.43	-0.21105	-73.5 ± 2.0	-79.8 ± 2.9
0.16896	0.01797	44.662	57.42 ± 0.38	60.11 ± 0.43	-0.23541	-69.2 ± 2.0	-75.4 ± 2.8

TABLE 2 The concentration dependences of relative densities, relative heat capacities, apparent molar volumes and apparent molar heat capacities for acidified aqueous solutions of $Gd(NO_3)_3$ at T = (288.15, 298.15, 313.15, and 328.15) K.

m_2 mol·kg^{-1}	m_3 mol·kg^{-1}	$\rho_{expt} - \rho_1$ kg·m^{-3}	$V_{\phi expt}$ cm^3·mol^{-1}	$V_{\phi 2}$ cm^3·mol^{-1}	$c_{p\,expt} - c_{p1}$ J·K^{-1}·g^{-1}	$C_{p\phi,expt}$ J·K^{-1}·mol^{-1}	$C_{p\phi 2}$ J·K^{-1}·mol^{-1}
T = 288.15 K							
0.01918	0.00037	5.678	47.00 ± 0.32	47.35 ± 0.38	-0.03285	-277.0 ± 3.8	-280.8 ± 4.3
0.03873	0.00075	11.426	47.74 ± 0.23	48.11 ± 0.30	-0.06518	-258.5 ± 2.1	-262.1 ± 2.9
0.05782	0.00111	17.013	48.25 ± 0.21	48.62 ± 0.29	-0.09593	-245.6 ± 1.6	-249.0 ± 2.6
0.07778	0.00150	22.842	48.53 ± 0.20	48.91 ± 0.28	-0.12730	-234.1 ± 1.4	-237.4 ± 2.4
0.09778	0.00188	28.641	48.97 ± 0.19	49.35 ± 0.28	-0.15788	-222.9 ± 1.3	-226.0 ± 2.4
0.11819	0.00228	34.534	49.38 ± 0.19	49.77 ± 0.28	-0.18857	-214.4 ± 1.2	-217.4 ± 2.3
0.13862	0.00267	40.440	49.53 ± 0.19	49.92 ± 0.27	-0.21845	-205.3 ± 1.2	-208.2 ± 2.3
0.15900	0.00306	46.242	50.10 ± 0.19	50.50 ± 0.27	-0.24769	-197.5 ± 1.1	-200.3 ± 2.3
0.18085	0.00348	52.492	50.35 ± 0.18	50.76 ± 0.27	-0.27854	-190.5 ± 1.1	-193.3 ± 2.3
0.20228	0.00390	58.660	50.29 ± 0.18	50.69 ± 0.27	-0.30824	-184.6 ± 1.1	-187.3 ± 2.3
T = 298.15 K							
0.01904	0.00037	5.573	49.73 ± 0.32	50.12 ± 0.38	-0.03158	-225.6 ± 3.8	-228.8 ± 4.3
0.03814	0.00073	11.134	50.31 ± 0.23	50.70 ± 0.30	-0.06218	-208.0 ± 2.1	-210.9 ± 2.9
0.05790	0.00111	16.853	50.86 ± 0.21	51.26 ± 0.29	-0.09303	-195.3 ± 1.6	-198.1 ± 2.6
0.07749	0.00149	22.492	51.36 ± 0.20	51.77 ± 0.28	-0.12267	-182.1 ± 1.4	-184.7 ± 2.4
0.09775	0.00188	28.298	51.80 ± 0.19	52.22 ± 0.28	-0.15300	-174.9 ± 1.3	-177.4 ± 2.4
0.11793	0.00227	34.052	52.20 ± 0.19	52.62 ± 0.28	-0.18235	-166.2 ± 1.2	-168.7 ± 2.3
0.13846	0.00267	39.891	52.52 ± 0.19	52.95 ± 0.27	-0.21165	-158.8 ± 1.1	-161.2 ± 2.3
0.15997	0.00308	45.990	52.80 ± 0.18	53.23 ± 0.27	-0.24145	-150.0 ± 1.1	-152.2 ± 2.3
0.18082	0.00348	51.881	53.04 ± 0.18	53.48 ± 0.27	-0.27009	-144.3 ± 1.1	-146.4 ± 2.3
0.20228	0.00390	57.913	53.31 ± 0.18	53.75 ± 0.27	-0.29885	-138.1 ± 1.0	-140.2 ± 2.3
T = 313.15 K							
0.01931	0.00037	5.579	52.39 ± 0.32	52.80 ± 0.38	-0.03109	-178.1 ± 3.7	-180.7 ± 4.2
0.05811	0.00112	16.676	53.76 ± 0.21	54.19 ± 0.29	-0.09038	-144.3 ± 1.6	-146.4 ± 2.5
0.07803	0.00150	22.327	54.25 ± 0.20	54.69 ± 0.28	-0.11997	-136.8 ± 1.4	-138.8 ± 2.4
0.09801	0.00189	27.969	54.68 ± 0.19	55.13 ± 0.28	-0.14897	-129.5 ± 1.2	-131.4 ± 2.3
0.11642	0.00224	33.148	55.05 ± 0.19	55.50 ± 0.27	-0.17489	-120.7 ± 1.2	-122.6 ± 2.3
0.13779	0.00265	39.139	55.36 ± 0.19	55.82 ± 0.27	-0.20486	-115.8 ± 1.1	-117.6 ± 2.3
0.15840	0.00305	44.889	55.68 ± 0.18	56.15 ± 0.27	-0.23256	-107.0 ± 1.1	-108.6 ± 2.3
0.18068	0.00348	51.092	55.93 ± 0.18	56.41 ± 0.27	-0.26242	-101.5 ± 1.0	-103.1 ± 2.3
0.20228	0.00390	57.082	56.16 ± 0.18	56.64 ± 0.27	-0.29049	-95.0 ± 1.0	-96.6 ± 2.2
T = 328.15 K							
0.01966	0.00038	5.619	53.96 ± 0.32	54.38 ± 0.38	-0.03131	-159.5 ± 3.7	-161.8 ± 4.2
0.03961	0.00076	11.299	54.23 ± 0.23	54.66 ± 0.30	-0.06190	-140.5 ± 2.0	-142.6 ± 2.9
0.05746	0.00111	16.345	54.70 ± 0.21	55.13 ± 0.29	-0.08876	-132.1 ± 1.6	-134.1 ± 2.6
0.07682	0.00148	21.780	55.35 ± 0.20	55.79 ± 0.28	-0.11685	-118.5 ± 1.4	-120.3 ± 2.4

0.09723	0.00187	27.487	55.83 ± 0.19	56.29 ± 0.28	-0.14621	-111.4 ± 1.2	-113.1 ± 2.3
0.11829	0.00228	33.370	56.11 ± 0.19	56.57 ± 0.28	-0.17525	-99.4 ± 1.1	-100.9 ± 2.3
0.13828	0.00266	38.906	56.53 ± 0.19	57.00 ± 0.27	-0.20318	-96.8 ± 1.1	-98.3 ± 2.3
0.15891	0.00306	44.642	56.63 ± 0.18	57.10 ± 0.27	-0.23005	-84.6 ± 1.1	-86.0 ± 2.3
0.18012	0.00347	50.461	57.05 ± 0.18	57.53 ± 0.27	-0.25857	-82.4 ± 1.0	-83.8 ± 2.2
0.20228	0.00390	56.561	57.23 ± 0.18	57.71 ± 0.27	-0.28709	-76.1 ± 1.0	-77.4 ± 2.2

TABLE 3 The concentration dependences of relative densities, relative heat capacities, apparent molar volumes and apparent molar heat capacities for acidified aqueous solutions of $Y(NO_3)_3$ at T = (288.15, 298.15, 313.15, and 328.15) K.

m_2 mol·kg^{-1}	m_3 mol·kg^{-1}	$\rho_{expt} - \rho_1$ kg·m^{-3}	$V_{\phi expt}$ cm^3·mol^{-1}	$V_{\phi 2}$ cm^3·mol^{-1}	$c_{p\ expt} - c_{p1}$ J·K^{-1}·g^{-1}	$C_{p\phi,expt}$ J·K^{-1}·mol^{-1}	$C_{p\phi 2}$ J·K^{-1}·mol^{-1}
T = 288.15 K							
0.01742	0.00041	4.000	45.40 ± 0.43	45.80 ± 0.48	-0.02501	-279.1 ± 4.4	-283.8 ± 4.9
0.03539	0.00083	8.097	45.99 ± 0.36	46.40 ± 0.41	-0.04992	-261.1 ± 2.8	-265.5 ± 3.4
0.05300	0.00124	12.083	46.57 ± 0.34	46.99 ± 0.39	-0.07370	-248.1 ± 2.4	-252.3 ± 3.1
0.07047	0.00165	16.026	46.97 ± 0.33	47.39 ± 0.39	-0.09672	-236.7 ± 2.2	-240.7 ± 3.0
0.08947	0.00210	20.286	47.40 ± 0.33	47.83 ± 0.38	-0.12131	-227.1 ± 2.1	-231.0 ± 2.9
0.10801	0.00254	24.426	47.78 ± 0.32	48.22 ± 0.38	-0.14501	-220.5 ± 2.0	-224.3 ± 2.9
0.12585	0.00295	28.406	48.01 ± 0.32	48.46 ± 0.38	-0.16741	-214.5 ± 2.0	-218.2 ± 2.8
0.14501	0.00340	32.654	48.31 ± 0.32	48.76 ± 0.37	-0.19083	-206.8 ± 2.0	-210.5 ± 2.8
0.16351	0.00384	36.766	48.43 ± 0.32	48.89 ± 0.37	-0.21290	-199.2 ± 1.9	-202.7 ± 2.8
0.18313	0.00430	41.082	48.72 ± 0.31	49.18 ± 0.37	-0.23595	-192.2 ± 1.9	-195.6 ± 2.8
T = 298.15 K							
0.01816	0.00043	4.102	48.66 ± 0.42	49.11 ± 0.47	-0.02490	-217.3 ± 4.3	-221.0 ± 4.7
0.03567	0.00084	8.027	49.28 ± 0.35	49.73 ± 0.40	-0.04810	-202.0 ± 2.7	-205.4 ± 3.4
0.05308	0.00125	11.903	49.84 ± 0.33	50.31 ± 0.39	-0.07078	-193.4 ± 2.3	-196.8 ± 3.0
0.07119	0.00167	15.921	50.24 ± 0.32	50.71 ± 0.38	-0.09371	-182.9 ± 2.1	-186.1 ± 2.9
0.09005	0.00211	20.085	50.63 ± 0.32	51.11 ± 0.38	-0.11703	-172.7 ± 2.0	-175.7 ± 2.8
0.10734	0.00252	23.902	50.79 ± 0.32	51.28 ± 0.37	-0.13817	-166.3 ± 1.9	-169.2 ± 2.8
0.12624	0.00296	28.028	51.21 ± 0.31	51.70 ± 0.37	-0.16110	-161.7 ± 1.9	-164.6 ± 2.8
0.14484	0.00340	32.093	51.43 ± 0.31	51.93 ± 0.37	-0.18289	-154.4 ± 1.9	-157.2 ± 2.7
0.16277	0.00382	36.006	51.59 ± 0.31	52.09 ± 0.37	-0.20323	-146.1 ± 1.9	-148.8 ± 2.7
T = 313.15 K							
0.01832	0.00043	4.072	51.40 ± 0.42	51.88 ± 0.46	-0.02436	-177.4 ± 4.2	-180.6 ± 4.7
0.03569	0.00084	7.908	51.89 ± 0.35	52.37 ± 0.40	-0.04659	-159.6 ± 2.7	-162.5 ± 3.3
0.05314	0.00125	11.732	52.47 ± 0.33	52.97 ± 0.39	-0.06836	-146.9 ± 2.2	-149.5 ± 3.0
0.07167	0.00168	15.775	52.91 ± 0.32	53.41 ± 0.38	-0.09102	-137.0 ± 2.0	-139.5 ± 2.9
0.08941	0.00210	19.632	53.22 ± 0.32	53.74 ± 0.37	-0.11234	-129.5 ± 1.9	-131.8 ± 2.8
0.10744	0.00252	23.528	53.57 ± 0.31	54.09 ± 0.37	-0.13361	-122.8 ± 1.9	-125.1 ± 2.7
0.12620	0.00296	27.573	53.84 ± 0.31	54.37 ± 0.37	-0.15539	-116.6 ± 1.8	-118.8 ± 2.7
0.14484	0.00340	31.579	54.08 ± 0.31	54.61 ± 0.37	-0.17679	-111.9 ± 1.8	-114.1 ± 2.7
0.16321	0.00383	35.524	54.23 ± 0.31	54.76 ± 0.37	-0.19754	-107.5 ± 1.8	-109.6 ± 2.7
0.18313	0.00430	39.758	54.53 ± 0.30	55.08 ± 0.36	-0.21948	-101.9 ± 1.7	-103.9 ± 2.7
T = 328.15 K							
0.01834	0.00043	4.030	52.77 ± 0.42	53.26 ± 0.47	-0.02407	-159.5 ± 4.2	-162.4 ± 4.6
0.03580	0.00084	7.853	52.99 ± 0.35	53.49 ± 0.40	-0.04609	-140.8 ± 2.7	-143.3 ± 3.3
0.05233	0.00123	11.435	53.61 ± 0.33	54.12 ± 0.39	-0.06637	-127.8 ± 2.2	-130.0 ± 3.0
0.06968	0.00164	15.182	54.05 ± 0.32	54.57 ± 0.38	-0.08729	-118.0 ± 2.0	-120.2 ± 2.9

0.08662	0.00203	18.829	54.35 ± 0.32	54.87 ± 0.38	-0.10738	-110.7 ± 1.9	-112.7 ± 2.8
0.10540	0.00247	22.844	54.76 ± 0.31	55.29 ± 0.37	-0.12922	-103.4 ± 1.9	-105.3 ± 2.7
0.12409	0.00291	26.840	54.97 ± 0.31	55.51 ± 0.37	-0.15044	-95.8 ± 1.8	-97.6 ± 2.7
0.14359	0.00337	30.981	55.27 ± 0.31	55.81 ± 0.37	-0.17220	-88.8 ± 1.8	-90.5 ± 2.7
0.16259	0.00382	34.988	55.60 ± 0.31	56.15 ± 0.37	-0.19324	-84.0 ± 1.7	-85.7 ± 2.7
0.18313	0.00430	39.362	55.61 ± 0.31	56.16 ± 0.36	-0.21561	-79.2 ± 1.7	-80.8 ± 2.6

TABLE 4 The concentration dependences of relative densities, relative heat capacities, apparent molar volumes and apparent molar heat capacities for aqueous solutions of $Ho(NO_3)_3$ at T = (288.15, 298.15, and 313.15) K.

m_2 mol·kg^{-1}	$\rho_{expt} - \rho_1$ kg·m^{-3}	$V_{\phi 2}$ cm^3·mol^{-1}	$c_{p\,expt} - c_{p1}$ J·K^{-1}·g^{-1}	$C_{p\phi 2}$ J·K^{-1}·mol^{-1}
T = 288.15 K				
0.02088	6.355	46.05 ± 0.24	-0.03618	-276.5 ± 3.6
0.05952	17.997	47.50 ± 0.08	-0.09998	-245.8 ± 1.8
0.10547	31.724	48.39 ± 0.04	-0.17066	-209.1 ± 1.4
0.15404	46.107	49.13 ± 0.03	-0.24339	-196.4 ± 1.3
0.16032	47.988	49.03 ± 0.03	-0.25247	-194.4 ± 1.3
0.24591	72.948	50.40 ± 0.02	-0.36970	-164.2 ± 1.2
0.28433	84.088	50.72 ± 0.01	-0.42076	-158.5 ± 1.2
0.32607	96.069	51.18 ± 0.01	-0.47264	-146.4 ± 1.2
0.37471	109.904	51.74 ± 0.01	-0.53061	-133.3 ± 1.1
0.43502	126.948	52.27 ± 0.01	-0.59980	-120.3 ± 1.1
T = 298.15 K				
0.02344	7.040	49.54 ± 0.21	-0.03879	-201.4 ± 3.3
0.08649	25.751	51.18 ± 0.05	-0.13730	-168.8 ± 1.5
0.13823	40.920	52.06 ± 0.03	-0.21354	-153.1 ± 1.4
0.18679	55.035	52.69 ± 0.02	-0.28099	-136.3 ± 1.3
0.23106	67.807	53.17 ± 0.02	-0.34022	-125.1 ± 1.3
0.28556	83.367	53.81 ± 0.01	-0.40896	-108.9 ± 1.2
0.33761	98.134	54.25 ± 0.01	-0.47248	-98.6 ± 1.2
0.38979	112.794	54.70 ± 0.01	-0.53261	-86.6 ± 1.1
0.43508	125.404	55.11 ± 0.01	-0.58280	-77.4 ± 1.1
0.48568	139.367	55.56 ± 0.01	-0.63629	-66.7 ± 1.1
T = 313.15 K				
0.08356	24.434	55.31 ± 0.06	-0.12901	-123.0 ± 1.5
0.13936	40.631	55.28 ± 0.03	-0.20889	-105.9 ± 1.3
0.18709	54.180	56.45 ± 0.02	-0.27300	-88.7 ± 1.3
0.23154	66.937	56.25 ± 0.02	-0.33051	-77.1 ± 1.2
0.28627	82.349	56.79 ± 0.01	-0.39866	-66.2 ± 1.2
0.33408	95.687	57.25 ± 0.01	-0.45521	-56.0 ± 1.1
0.39272	111.855	57.86 ± 0.01	-0.52136	-44.2 ± 1.1
0.43684	123.986	58.13 ± 0.01	-0.57001	-38.5 ± 1.1
0.48228	136.365	58.46 ± 0.01	-0.61581	-26.7 ± 1.1

TABLE 5 The concentration dependences of relative densities, relative heat capacities, apparent molar volumes and apparent molar heat capacities for aqueous solutions of $Y(NO_3)_3$ at T = (288.15, 298.15, 313.15, and 328.15) K.

m_2 mol·kg^{-1}	$\rho_{expt} - \rho_1$ kg·m^{-3}	$V_{\phi 2}$ cm^3·mol^{-1}	$c_{p\,expt} - c_{p1}$ J·K^{-1}·g^{-1}	$C_{p\phi 2}$ J·K^{-1}·mol^{-1}
T = 288.15 K				
0.02552	5.820	46.39 ± 0.19	-0.03636	-284.3 ± 2.8
0.04399	9.992	47.16 ± 0.11	-0.06144	-262.7 ± 1.8
0.09000	20.285	48.39 ± 0.05	-0.12100	-226.9 ± 1.1
0.13290	29.813	48.99 ± 0.03	-0.17472	-211.9 ± 0.9
0.18461	41.146	49.84 ± 0.02	-0.23610	-193.0 ± 0.8
0.22823	50.625	50.40 ± 0.02	-0.28610	-181.5 ± 0.8
0.27585	60.890	50.93 ± 0.01	-0.33681	-162.8 ± 0.7
0.33408	73.321	51.52 ± 0.01	-0.39808	-150.3 ± 0.7
0.38722	84.531	52.07 ± 0.01	-0.44950	-133.6 ± 0.7
0.44185	96.008	52.45 ± 0.01	-0.50071	-120.1 ± 0.7
T = 298.15 K				
0.03894	8.705	50.41 ± 0.13	-0.05195	-199.5 ± 1.9
0.07894	17.541	51.31 ± 0.06	-0.10244	-176.9 ± 1.1
0.11748	25.973	51.99 ± 0.04	-0.14933	-163.2 ± 0.9
0.15817	34.833	52.38 ± 0.03	-0.19715	-151.7 ± 0.8
0.19821	43.424	53.05 ± 0.02	-0.24169	-136.9 ± 0.8
0.23521	51.344	53.40 ± 0.02	-0.28243	-129.4 ± 0.7
0.27747	60.310	53.84 ± 0.01	-0.32684	-118.8 ± 0.7
0.32132	69.547	54.23 ± 0.01	-0.37055	-106.1 ± 0.7
0.37064	79.837	54.68 ± 0.01	-0.41897	-96.6 ± 0.7
0.41718	89.484	55.03 ± 0.01	-0.46181	-85.0 ± 0.7
T = 313.15 K				
0.03280	7.228	52.87 ± 0.15	-0.04252	-163.4 ± 2.2
0.06997	15.332	53.70 ± 0.07	-0.08851	-140.5 ± 1.2
0.10603	23.106	54.46 ± 0.04	-0.13087	-121.5 ± 1.0
0.15588	33.766	55.18 ± 0.03	-0.18748	-105.5 ± 0.8
0.19138	41.291	55.62 ± 0.02	-0.22652	-97.2 ± 0.8
0.24872	53.331	56.26 ± 0.02	-0.28633	-81.2 ± 0.7
0.31261	66.611	56.83 ± 0.01	-0.35105	-70.8 ± 0.7
0.36783	77.972	57.26 ± 0.01	-0.40255	-56.3 ± 0.7
0.43242	91.110	57.76 ± 0.01	-0.46217	-47.2 ± 0.6
0.48380	101.452	58.13 ± 0.01	-0.50554	-35.2 ± 0.6
T = 328.15 K				
0.02501	5.466	53.63 ± 0.20	-0.03198	-140.4 ± 2.9
0.06702	14.534	54.92 ± 0.07	-0.08328	-115.7 ± 1.2
0.12907	27.750	56.05 ± 0.04	-0.15519	-95.3 ± 0.9
0.19543	41.688	56.96 ± 0.02	-0.22669	-72.5 ± 0.7

0.23989	50.923	57.46 ± 0.02	-0.27262	-61.6 ± 0.7
0.30162	63.634	58.02 ± 0.01	-0.33360	-48.0 ± 0.7
0.33230	69.886	58.32 ± 0.01	-0.36328	-43.4 ± 0.7
0.37529	78.595	58.69 ± 0.01	-0.40232	-32.9 ± 0.6
0.43337	90.259	59.14 ± 0.01	-0.45428	-23.4 ± 0.6
0.50327	104.119	59.68 ± 0.01	-0.51392	-12.7 ± 0.6

TABLE 6 Estimates of parameters to the Pitzer ion interaction model equations, shown as equations (6) and (9) within the text, for aqueous solutions of $Pr(NO_3)_3$, $Gd(NO_3)_3$, $Ho(NO_3)_3$, and $Y(NO_3)_3$ at T = (288.15, 298.15, 313.15, and 328.15) K and p = 0.1 MPa.

T / K	V^{o}_2 / $cm^3 \cdot mol^{-1}$	$10^4 \cdot \beta^{0V}$ / $cm^3 \cdot kg \cdot mol^{-1} \cdot J^{-1}$	$10^3 \cdot \beta^{1V}$ / $cm^3 \cdot kg \cdot mol^{-1} \cdot J^{-1}$	$C_p^{o}{}_2$ / $J \cdot K^{-1} \cdot mol^{-1}$	$10^5 \cdot \beta^{0J}$ / $kg \cdot mol^{-1} \cdot K^{-2}$	$10^4 \cdot \beta^{1J}$ / $kg \cdot mol^{-1} \cdot K^{-2}$
			$Pr(NO_3)_3$			
288.15	43.32 ± 0.10	-1.552 ± 1.433	3.966 ± 0.579	-376.9 ± 3.7	1.837 ± 1.793	-3.583 ± 0.724
298.15	46.97 ± 0.07	-2.662 ± 0.986	2.686 ± 0.398	-321.7 ± 3.3	1.530 ± 1.472	-2.348 ± 0.594
313.15	48.33 ± 0.21	-8.092 ± 2.635	4.853 ± 1.065	-268.9 ± 1.1	-0.951 ± 0.426	-0.525 ± 0.173
328.15	50.60 ± 0.08	-4.974 ± 0.951	1.270 ± 0.382	-237.7 ± 1.5	1.264 ± 0.559	-0.317 ± 0.225
			$Gd(NO_3)_3$			
288.15	44.84 ± 0.23	3.136 ± 2.393	-2.482 ± 1.078	-331.8 ± 1.2	-2.755 ± 0.444	-0.305 ± 0.200
298.15	47.33 ± 0.13	3.618 ± 1.351	-2.919 ± 0.608	-282.8 ± 1.5	-2.032 ± 0.519	0.412 ± 0.234
313.15	49.63 ± 0.08	1.470 ± 0.718	-2.825 ± 0.326	-238.6 ± 2.8	-0.913 ± 0.820	0.886 ± 0.373
328.15	50.93 ± 0.32	5.244 ± 2.982	-6.062 ± 1.347	-226.5 ± 3.9	-1.292 ± 1.095	1.373 ± 0.495
			$Y(NO_3)_3$			
288.15	43.22 ± 0.12	1.879 ± 1.497	-1.795 ± 0.630	-331.6 ± 1.9	-2.079 ± 0.797	-0.349 ± 0.336
298.15	46.42 ± 0.11	1.782 ± 1.582	-2.595 ± 0.627	-269.4 ± 2.7	-3.818 ± 1.242	1.520 ± 0.492
313.15	48.88 ± 0.13	2.472 ± 1.469	-3.942 ± 0.621	-240.4 ± 0.7	1.198 ± 0.251	0.157 ± 0.106
328.15	49.91 ± 0.28	4.212 ± 2.968	-5.919 ± 1.256	-227.3 ± 1.0	0.379 ± 0.342	0.695 ± 0.145
			***$Ho(NO_3)_3$**			
288.15	43.43 ± 0.13	2.969 ± (0.466)	-2.031 ± 0.353	-332.3 ± 4.7	-1.923 ± 0.595	-0.991 ± 0.451
298.15	46.61 ± 0.04	2.033 ± (0.122)	-2.579 ± 0.104	-262.9 ± 2.6	1.278 ± 0.523	-0.038 ± 0.008
313.15	51.88 ± 0.90	2.962 ±1.486	-6.672 ±1.665	-221.5 ± 6.1	-1.339 ± 0.321	1.252 ± 0.360
			***$Y(NO_3)_3$**			
288.15	43.40 ± 0.08	1.987 ± 0.290	-1.221 ± 0.222	-342.1 ± 4.6	-2.542 ± 0.582	-0.869 ± 0.058
298.15	46.96 ± 0.11	1.918 ± 0.352	-2.773 ± 0.286	-264.1 ± 2.5	-2.636 ± 0.251	1.310 ± 0.205
313.15	49.11 ± 0.10	0.873 ± 0.246	-3.105 ± 0.218	-235.2 ± 2.8	-1.035 ± 0.230	0.910 ± 0.204
328.15	49.79 ± 0.04	0.562 ± 0.112	-3.910 ± 0.096	-208.2 ± 2.5	-1.145 ± 0.198	1.776 ± 0.169

* Aqueous solutions of nitrate salt obtained from LLNL.

TABLE 7. Coefficients to equation (8) that models the temperature dependences of V^{o}_{2} values at p = 0.1 MPa.

Coefficient	$Pr(NO_3)_3$(aq)	$Gd(NO_3)_3$(aq)	$Y(NO_3)_3$(aq)
a /($cm^3 \cdot mol^{-1}$)	49.03 ± 0.09_5	48.99 ± 0.08	48.3 ± 0.1
b/($cm^3 \cdot mol^{-1} \cdot K^{-1}$)	0.176 ± 0.003	0.146 ± 0.008	0.160 ± 0.007
$10^3 \cdot c$/($cm^3 \cdot mol^{-1} \cdot K^{-2}$)	-5.0 ± 0.3	-2.8 ± 0.6	-4.6 ± 0.5

Coefficient	*$Y(NO_3)_3$(aq)
a /($cm^3 \cdot mol^{-1}$)	48.69 ± 0.09
b/($cm^3 \cdot mol^{-1} \cdot K^{-1}$)	0.157 ± 0.002
$10^3 \cdot c$/($cm^3 \cdot mol^{-1} \cdot K^{-2}$)	-5.1 ± 0.3

* Aqueous solutions of nitrate salt obtained from LLNL.

TABLE 8. Comparison of calculated V_2^o and $C_p^o{}_2$ values with those previously reported in the literature for aqueous solutions of $Pr(NO_3)_3$, $Gd(NO_3)_3$, $Y(NO_3)_3$, and $Ho(NO_3)_3$ at T = 298.15 K and p = 0.1 MPa.

	V_2^o / cm^3·mol^{-1}	$C_p^o{}_2$ / J·K^{-1}·mol^{-1}
$Pr(NO_3)_3$	46.97 (0.07), 46.03 (0.23)[a], 45.524[b], 45.20[c], 45.46[d]	-321.7 (3.3), -299.91[e], -327.09[f]
$Gd(NO_3)_3$	47.33 (0.13), 47.22 (0.05)[a], 47.126[b], 46.73[c], 47.00[d]	-282.8 (1.5), -243.17[e], -288.18[f]
$Y(NO_3)_3$	46.42 (0.11), 46.96 (0.11), 54.78[g]	-269.4 (2.7), -264.1 (2.5)
$Ho(NO_3)_3$	46.61 (0.04), 45.54 (0.10)[a], 45.768[b], 46.05[c], 45.66[d]	-262.9 (2.6), -237.82[e], -308.00[f]

[a]Ref. 1.

[b]Ref. 13.

[c]Calculated using the empirical equation for V_2^o that is reported in Ref. 11.

[d]Calculated using the Owen-Brinkley equation that is reported in Ref. 11.

[e]Ref. 14.

[f]Table III of Ref. 25.

[g]Ref. 24.

TABLE 9. Estimates of parameters to equations (10), (11), and (12) which model the temperature dependences of $V_{\phi,2}$ values for aqueous solutions of $Pr(NO_3)_3$(aq), $Gd(NO_3)_3$(aq), $Y(NO_3)_3$(aq), *$Y(NO_3)_3$(aq), and *$Ho(NO_3)_3$(aq) at p = 0.1 MPa.

Parameter	$Pr(NO_3)_3$	$Gd(NO_3)_3$	$Y(NO_3)_3$	*$Y(NO_3)_3$	*$Ho(NO_3)_3$
υ_1 /($cm^3 \cdot mol^{-1}$)	82.82 ± 0.38	81.93 ± 0.33	83.72 ± 0.45	83.38 ± 0.28	85.64 ± 1.24
$10^{-1} \cdot \upsilon_2$ /($cm^3 \cdot K \cdot mol^{-1}$)	145.97 ± 2.61	-130.49 ± 2.18	-151.09 ± 3.36	-147.33 ± 2.06	-161.13 ± 8.61
$10^4 \cdot \upsilon_3$ /($kg \cdot mol^{-1} \cdot MPa^{-1}$)	51.53 ± 9.48	58.82 ± 6.50	-24.44 ± 20.15	8.58 ± 3.56	42.74 ± 15.61
$10^6 \cdot \upsilon_4$ /($kg \cdot mol^{-1} \cdot K^{-1} \cdot MPa^{-1}$)	-18.19 ± 2.81	-18.02 ± 1.95	8.77 ± 6.51	-2.42 ± 1.14	-13.69 ± 5.17
υ_5 /($kg \cdot mol^{-1} \cdot K \cdot MPa^{-1}$)	0.97 ± 0.28	-1.11 ± 0.20	-9.03 ± 6.47	7.07 ± 0.84	56.23 ± 20.50
$10 \cdot \upsilon_6$ /($kg \cdot mol^{-1} \cdot MPa^{-1}$)	-	-	0.91 ± 0.37	-0.26 ± 0.03	-3.70 ± 1.33
$10^4 \cdot \upsilon_7$ /($kg \cdot mol^{-1} \cdot K^{-1} \cdot MPa^{-1}$)	-	-	-2.10 ± 0.56	-	6.00 ± 2.17
Stand. Error ($cm^3 \cdot mol^{-1}$)	0.21	0.17	0.10	0.082	0.22

* Aqueous solutions of nitrate salt obtained from LLNL.

TABLE 10. Estimates of parameters to equations (13), (14), and (15) which model the temperature dependences of $C_{p\phi,2}$ values for aqueous solutions of $Pr(NO_3)_3$(aq), $Gd(NO_3)_3$(aq), $Y(NO_3)_3$(aq), *$Y(NO_3)_3$(aq), and *$Ho(NO_3)_3$(aq) at p = 0.1 MPa.

Parameter	$Pr(NO_3)_3$	$Gd(NO_3)_3$	$Y(NO_3)_3$	*$Y(NO_3)_3$	*$Ho(NO_3)_3$
c_1 /(J·K^{-1}·mol^{-1})	88.96 ± 5.39	91.33 ± 4.58	97.52 ± 3.28	127.38 ± 5.91	165.43 ± 9.19
$10^{-5}\cdot c_2$ /(J·K·mol^{-1})	-9.30 ± 0.28	-7.50 ± 0.23	-7.57 ± 0.17	-9.00 ± 0.03	-9.95 ± 0.42
$10\cdot c_3$ /(kg·mol^{-1}·K^{-1})	37.81 ± 8.47	-8.19 ± 1.22	-18.73 ± 4.53	-3.32 ± 2.49	-15.97 ± 2.02
$10^{3}\cdot c_4$ /(kg·mol^{-1}·K^{-2})	-24.64 ± 5.45	5.11 ± 0.83	11.97 ± 2.91	2.02 ± 1.61	10.53 ± 1.35
$10^{6}\cdot c_5$ /(kg·mol^{-1}·K^{-3})	40.08 ± 8.76	-7.98 ± 1.43	-19.09 ± 4.68	-3.10 ± 2.58	-17.42 ± 2.26
c_6 /(kg·mol^{-1}·K^{-1})	-17.37 ± 2.68	-0.25 ± 0.14	3.29 ± 1.48	-3.56 ± 1.42	-0.92 ± 0.17
$10^{2}\cdot c_7$ /(kg·mol^{-1}·K^{-2})	1.82 ± 0.28	0.014 ± 0.007	-0.37 ± 0.16	0.36 ± 0.15	0.053 ± 0.010
$10^{5}\cdot c_8$ /(kg·mol^{-1}·K^{-3})	-2.90 ± 0.45	-	0.61 ± 0.25	-0.53 ± 0.24	-
Stand. Error (J·K^{-1}·mol^{-1})	2.2	2.1	1.3	2.9	3.2

* Aqueous solutions of nitrate salt obtained from LLNL.

Figures

Figure 1. A plot of apparent molar volume, $V_{\phi,2}$, against the square root of the ionic strength, $I^{1/2}$, for aqueous solutions of $Pr(NO_3)_3$(aq) at T = 298.15 K and p = 0.1 MPa •, Ref. [13]; Δ, Ref. [11];○, this study (values obtained via Young's Rule from acidified solutions of the salt).

Figure 2. A plot of apparent molar volume, $V_{\phi,2}$, against the square root of the ionic strength, $I^{1/2}$, for aqueous solutions of $Y(NO_3)_3$(aq) at T = 298.15 K and p = 0.1 MPa O, Ref. [9]; •, this study (values obtained via Young's Rule from acidified solutions of the salt); Δ, this study (values obtained from aqueous solution obtained from LLNL).

Figure 3. A plot of $V_{2,\phi} - (6 \cdot A_v/b) \cdot \ln(1+bI^{1/2}) + \omega Q$ against the square root of ionic strength, $I^{1/2}$, for aqueous solutions of $Pr(NO_3)_3$(aq) at p = 0.1 MPa and •,T = 288.15 K; O, T = 298.15 K; ■, T = 313.15 K; □, T = 328.15 K.

Figure 4. A plot of $C_{p2,\phi} - (6 \cdot A_J/b) \cdot \ln(1+bI^{1/2}) - \omega TX$ against the square root of ionic strength, $I^{1/2}$, for aqueous solutions of $Ho(NO_3)_3$(aq) at p = 0.1 MPa and •,T = 288.15 K; O, T = 298.15 K; ■, T = 313.15 K.

Figure 5. A plot of $(V_{2,\phi} - V_2^o)$ against the square root of ionic strength, $I^{1/2}$, at T = 298.15 K and p = 0.1 MPa for aqueous solutions of • ,$Pr(ClO_4)_3$(aq); O, $Pr(NO_3)_3$(aq).

Figure 6. A plot of $(C_{p2,\phi} - C_{p2}^o)$ against the square root of ionic strength, $I^{1/2}$, at T = 298.15 K and p = 0.1 MPa for aqueous solutions of • ,$Pr(ClO_4)_3$(aq); O, $Pr(NO_3)_3$(aq).

Figure 7. $\{V^{o}_{2}(NO_3^-) - V^{0}_{2}(ClO_4^-)\}$ plotted against temperature for O, HNO_3(aq) and $HClO_4$(aq); □, $Pr(NO_3)_3$(aq) and $Pr(ClO_4)_3$(aq); ■, $Gd(NO_3)_3$(aq) and $Gd(ClO_4)_3$(aq); ◊, $Y(NO_3)_3$(aq) and $Y(ClO_4)_3$(aq); +, *$Y(NO_3)_3$(aq) and $Y(ClO_4)_3$(aq); Δ, *$Ho(NO_3)_3$(aq) and $Ho(ClO_4)_3$(aq). The solid line drawn through the $\{V^{o}_{2}(NO_3^-) - V^{0}_{2}(ClO_4^-)\}$ values for HNO_3(aq) and $HClO_4$(aq) is for visualization purposes only. (* LLNL solution)

Figure 8. $\{C_p{}^{o}_{2}(NO_3^-) - C_p{}^{0}_{2}(ClO_4^-)\}$ plotted against temperature for O, HNO_3(aq) and $HClO_4$(aq); □, $Pr(NO_3)_3$(aq) and $Pr(ClO_4)_3$(aq); ■, $Gd(NO_3)_3$(aq) and $Gd(ClO_4)_3$(aq); ◊, $Y(NO_3)_3$(aq) and $Y(ClO_4)_3$(aq); +, *$Y(NO_3)_3$(aq) and $Y(ClO_4)_3$(aq); Δ, *$Ho(NO_3)_3$(aq) and $Ho(ClO_4)_3$(aq). The solid line drawn through the $\{C_p{}^{o}_{2}(NO_3^-) - C_p{}^{0}_{2}(ClO_4^-)\}$ values for HNO_3(aq) and $HClO_4$(aq) is for visualization purposes only. (* LLNL solution)

Figure 1.

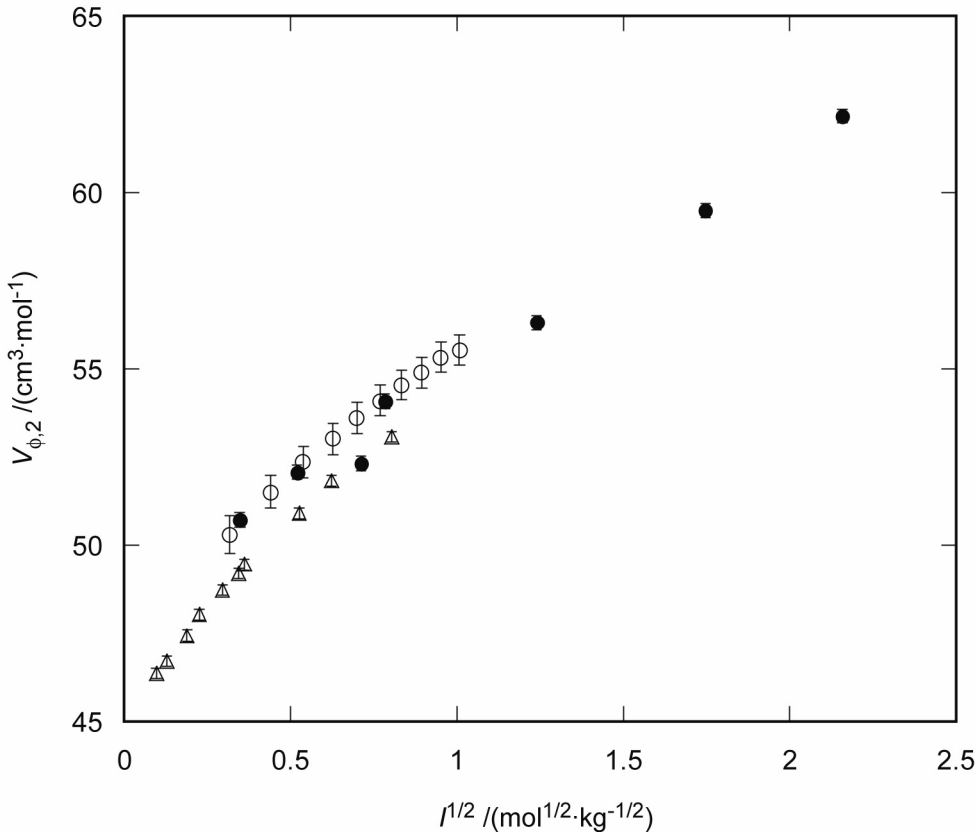

Figure 2.

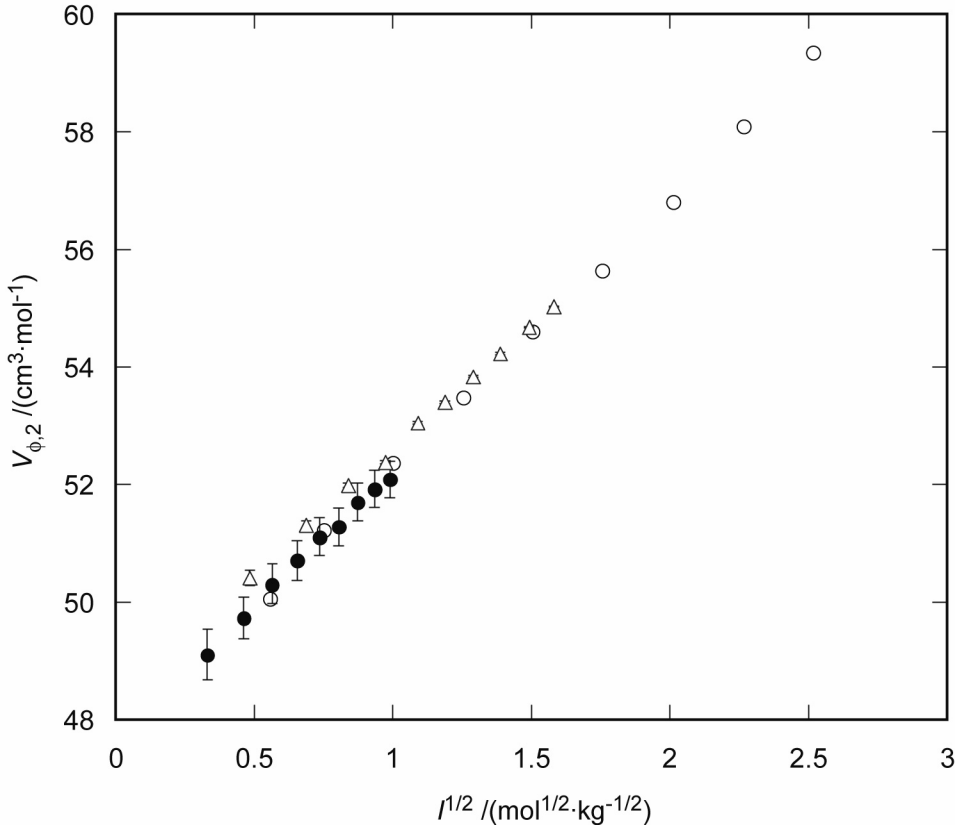

Figure 3.

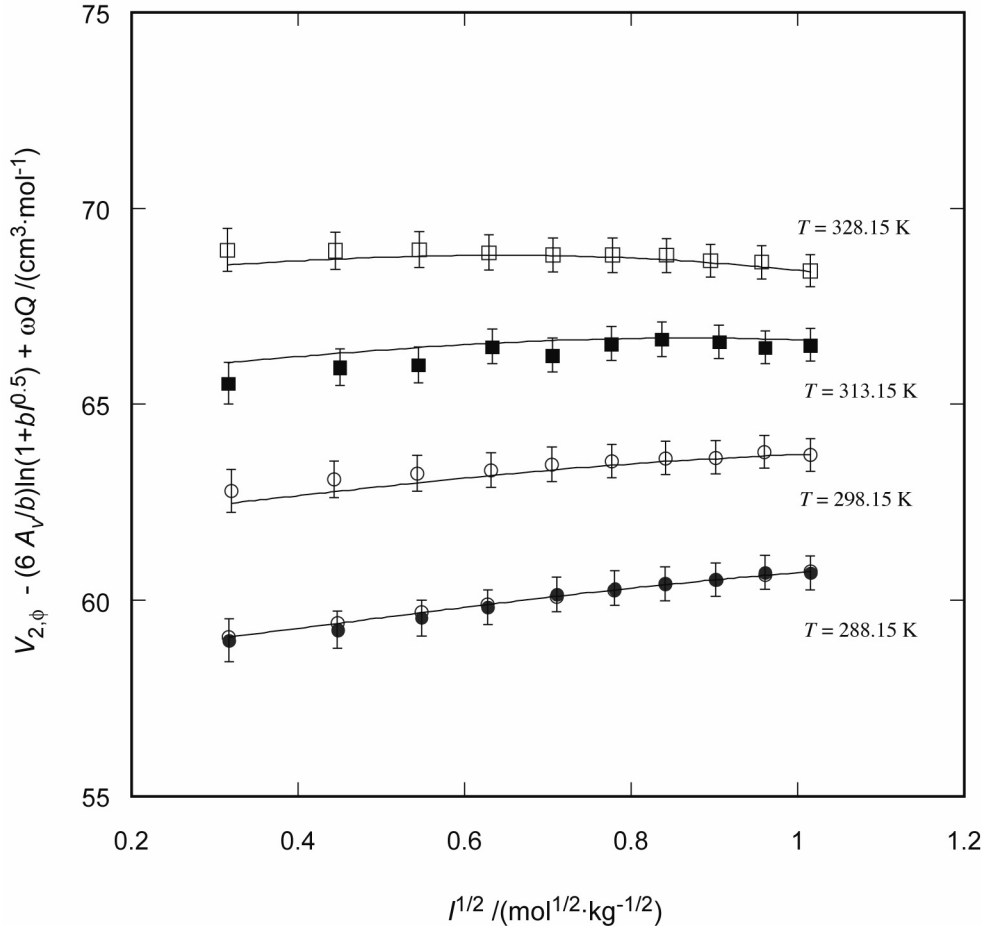
75
70
65
60
55
0.2
0.4
0.6
0.8
1
1.2
$V_{2,\phi}$ - (6 $A_V b$)ln(1+$bI^{0.5}$) + ωQ /(cm^3·mol^{-1})
$I^{1/2}$ /(mol$^{1/2}$·kg$^{-1/2}$)
T = 328.15 K
T = 313.15 K
T = 298.15 K
T = 288.15 K

Figure 4

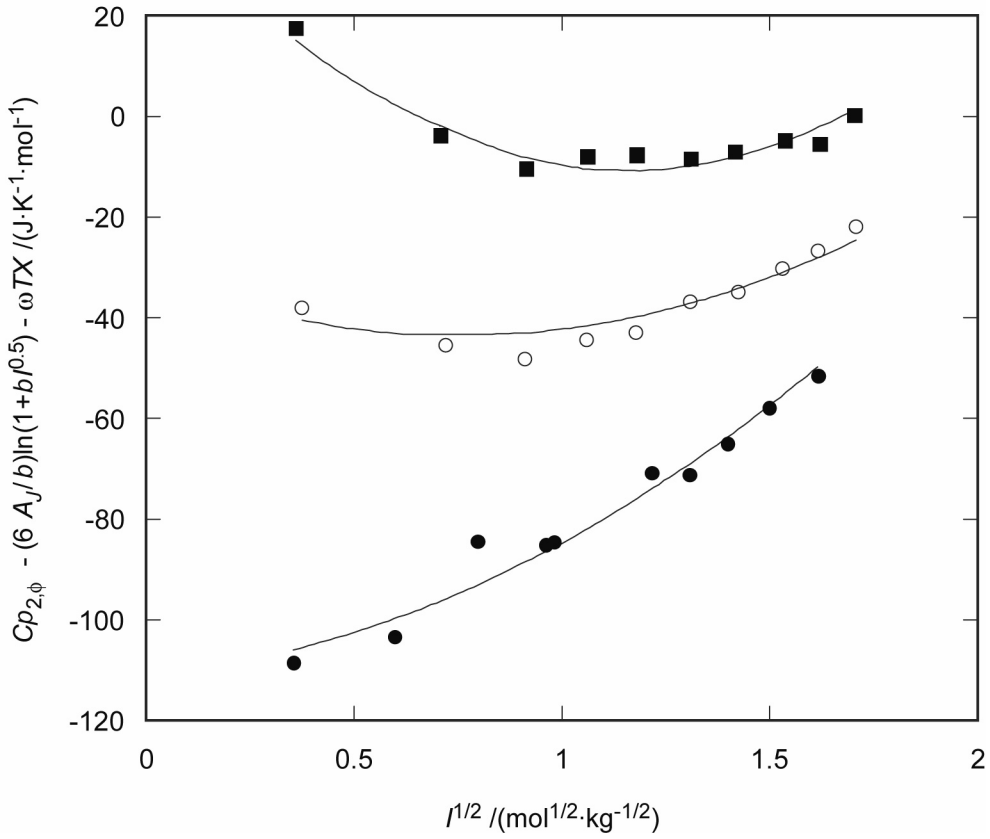
20
0
-20
-40
-60
-80
-100
-120
0
0.5
1
1.5
2
$Cp_{2,\phi}$ - (6 A_J/b)ln(1+$bI^{0.5}$) - ωTX /(J·K^{-1}·mol^{-1})
$I^{1/2}$ /(mol$^{1/2}$·kg$^{-1/2}$)

Figure 5

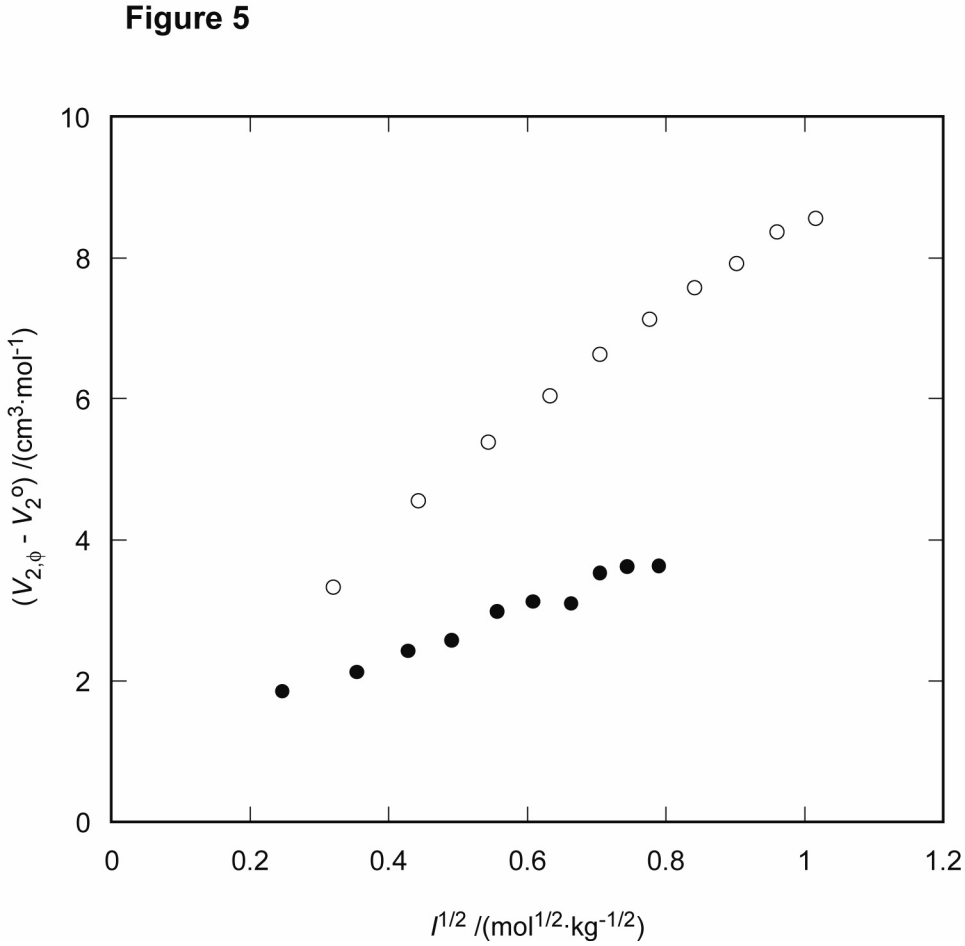

Figure 6.

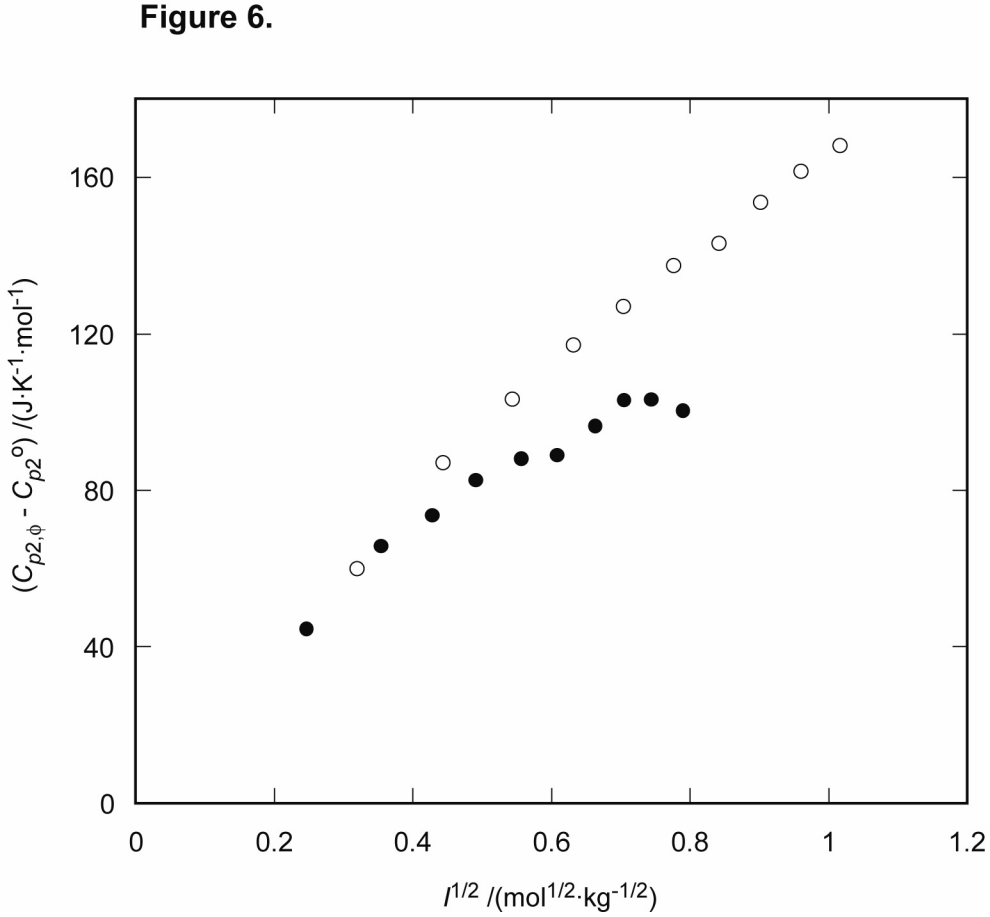
160
120
80
40
0
0
0.2
0.4
0.6
0.8
1
1.2
$(C_{p2,\phi} - C_{p2}^{o})$ /(J·K^{-1}·mol^{-1})
$I^{1/2}$ /(mol$^{1/2}$·kg$^{-1/2}$)

Figure 7.

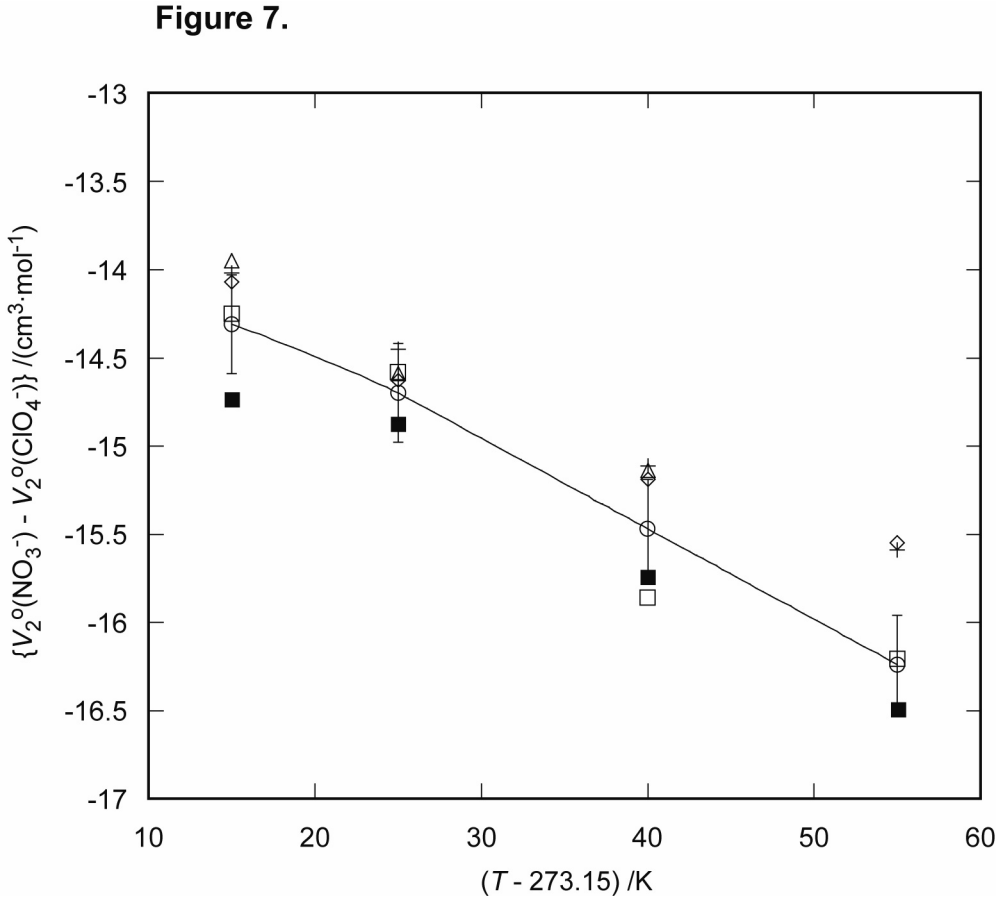
-13
-13.5
-14
-14.5
-15
-15.5
-16
-16.5
-17
10
20
30
40
50
60
{$V_2^o(NO_3^-)$ - $V_2^o(ClO_4^-)$} /(cm^3·mol^{-1})
(T - 273.15) /K

Figure 8.

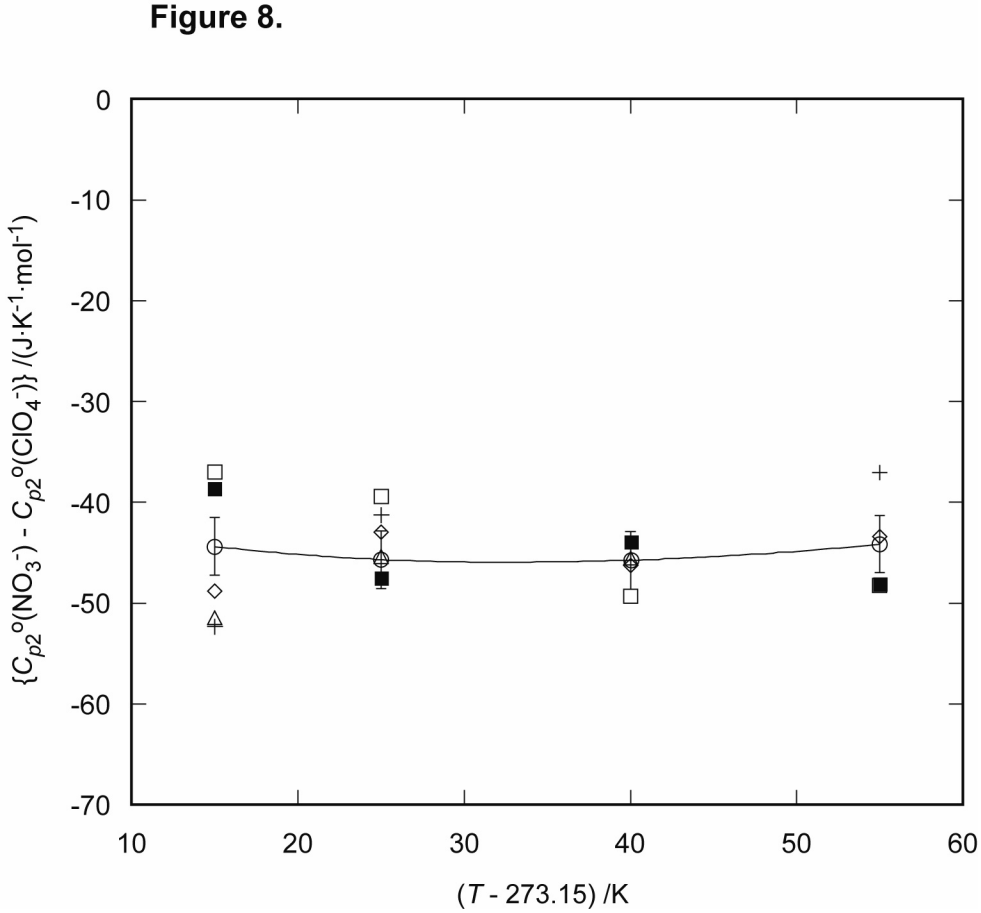
0
-10
-20
-30
-40
-50
-60
-70
10
20
30
40
50
60
{$C_{p2}^{o}(NO_3^-) - C_{p2}^{o}(ClO_4^-)$} /(J·K^{-1}·mol^{-1})
(T - 273.15) /K

University of California
Lawrence Livermore National Laboratory
Technical Information Department
Livermore, CA 94551